Universidad de Huelva

Departamento de Ciencias Integradas

Study of radon exhalation rates and its influence on ambient radon concentrations in the city of Huelva

Memoria para optar al grado de doctor
presentada por:

Isidoro Gutiérrez Álvarez

Fecha de lectura: 17 de diciembre de 2020

Bajo la dirección de los doctores:

Juan Pedro Bolívar Raya

José Enrique Martín Domínguez

José Antonio Adame Carnero

Huelva, 2020

STUDY OF RADON EXHALATION RATES AND ITS INFLUENCE ON AMBIENT RADON CONCENTRATIONS IN THE CITY OF HUELVA

PhD Thesis

1 DE SEPTIEMBRE DE 2020

ISIDORO GUTIÉRREZ ÁLVAREZ
Universidad de Huelva

A un pequeño llamado Ben,
who always wears the most precious smile

Agradecimientos

Personalmente, nunca estuvo en mis planes escribir algún día unas líneas de agradecimiento para mi tesis doctoral, lo cierto es que nunca pensé que llegaría a escribir una tesis en primer lugar. La oportunidad me vino por casualidad durante mi trabajo de fin de Máster, en el que tuve la suerte de contar con José Antonio Adame como tutor, quien me puso más tarde en contacto con Juan Pedro Bolívar y José Enrique Martín. A ellos tres les debo estos últimos años de mi vida, durante los que he tenido muchas más alegrías que tristezas y he aprendido mucho más que ciencia. Espero que me perdonéis que no os trate de Doctor y os dedique sólo un párrafo, pero como bien dicen la confianza da asco y unas líneas más seguirían sin bastar. Muchísimas gracias a los tres por todo vuestro tiempo, cariño y esfuerzo, y, sobre todo, por darme una oportunidad de las que sólo ocurren una vez en la vida.

Apenas había salido de las prácticas del Máster cuando Juan Pedro tuvo a bien asignarme una mesa en la sala de becarios de la cuarta planta. Mi yo del pasado no sabía aún que allí conocería a muchos a los que luego tendría por muy buenos amigos. Allí me los fueron presentando a todos como los expertos que eran: Fernando el experto en radiactividad, José Luis el experto en aguas, Silvia la experta en residuos y Angie la experta en aceleradores, que en realidad no pertenecía al grupo de investigación (allí no trabajamos con aceleradores) pero la queremos como una más. Poco tiempo duré como el novato, ya que rápidamente llegó Daniela, experta en alegrarme la mañana yendo a desayunar. Esa sala ha sido una segunda casa durante todo este tiempo y es gracias a ellos que se ha pasado volando. Mil gracias a todos por las risas, por vuestro apoyo y, sobre todo, por los cafés y las cervezas.

Con la idea de que aprendiera a medir radón en suelos, me mandaron unos días de estancia a la Universidad de Las Palmas de Gran Canaria, con el Dr. Héctor Alonso Hernández, el Dr. Jesús García Rubiano y con Jonay González, doctorando en aquel momento. No podía estar más de acuerdo con la idea. En Las Palmas no sólo aprendí de radón, que también, sino que disfruté de un entorno increíble gracias a mis anfitriones. Allí probé la que probablemente fuera la mejor hamburguesa que he comido en mi vida, además de ver casi todas las facetas de la isla de Las Palmas. Gracias a los tres por vuestro tiempo y vuestra hospitalidad.

Entretanto, comenzó lo que sería el núcleo de la parte experimental de la tesis: el diseño y experimentación con las cámaras de acumulación. Hubo que recoger material *in situ* (gracias Fer y JL por ayudarme a cargar) y hacer muchísimo trabajo de laboratorio. Aprendí a usar soldadores de estaño, empalmar cables, manejar sierras radiales y otras tantas cosas más propias de un taller que de un laboratorio. En este punto es necesario mencionar a Antonio Padilla, sin duda la mejor persona que he conocido durante esta etapa. Él me enseñó todo lo necesario para manejarme en el laboratorio y, no contento con eso, me siguió ayudando siempre que me hizo falta. Ésta y otras tantas tesis del departamento sólo han sido posibles gracias él. Mil gracias, Padi, de corazón.

Un buen verano, de esos con calor sofocante y sol de justicia, decidimos hacer una campaña de medida de tasas de exhalación de radón en las balsas de fosfoyeso. Para ello contamos con el Dr. Arturo Vargas y la Dra. Claudia Grossi, de la Universitat Politècnica de Catalunya. Fueron dos días de medidas bajo un sol abrasador (tuvimos que comprar un toldo para no arriesgarnos a morir de insolación). Pese a todo, resultó ser una muy buena experiencia, tanto laboral como personal. Arturo y Claudia, muchísimas gracias por compartir vuestros conocimientos y por dedicar vuestro tiempo y vuestra energía a mejorar en gran medida esta tesis.

Las visitas a las balsas se convirtieron en una rutina ya que había que hacer controles periódicos a los equipos para verificar que seguían funcionando bien. Para esto hubo que involucrar a mucha

gente: gracias de nuevo a José Enrique y a Antonio Padilla, que me ayudaron a instalar los equipos; a José Luis por acompañarme tantas veces a hacer la ronda; a la gente del departamento de Infraestructuras, que me prestaron más de una vez sus furgonetas cuando me hizo falta y a Manuel Ceada y Laureano Conejo, que me enseñaron a no perderme por aquellos lares. Gracias a todos.

Uno de los puntos de inflexión fue mi primera presentación oral en un congreso, que fue nada menos que en Verbania-Intra, situada en los Alpes italianos. Después de todo, una de las grandes ventajas del trabajo de investigador es que se viaja mucho. Al ser un congreso internacional, mi primera presentación oral sobre mi trabajo personal como investigador, debía de ser en inglés. Practiqué tanto esa presentación que la hice en modo automático, tanto que después no recordaba ciertas partes de la misma. Allí coincidí de nuevo con Jesús García Rubiano, de la mano del cual conocí a otros veteranos en el estudio del radón, como son el Dr. Luis Quindós y Lluís Font. A ambos debo agradecerles sus valiosos consejos, ya que me resolvieron muchas dudas y me dieron algunas buenas ideas. Quisiera mencionar especialmente a Lluís Font. Hacer una tesis puede ser abrumador, pero también emocionante, y Lluís es capaz de transmitir ese tipo de entusiasmo que te hace disfrutar un poco más de la investigación. Gracias a todos ellos.

Durante la tesis realicé varias estancias, la primera de ellas en el instituto Max Planck de Química en Maguncia, Alemania, de la mano del Dr. Hartwig Harder y su grupo. No es exagerado decir que allí subí mi nivel de programación un par de órdenes de magnitud. Aprendí a usar Git, cambié de Spyder a Visual Code Studio y escribí más de 2000 mil líneas de código para manejar el modelo FLEXPART. Todo ello gracias a la orientación de Hartwig y al buen ambiente que allí tenían. Mil gracias a Hartwig, Anywhere, Carolina y al resto del grupo, que me trataron como a uno más e hicieron que un mes en Alemania durara tanto como un suspiro.

Para la segunda estancia volví a visitar a viejos amigos en la Estación de Sondeos Atmosféricos del INTA. Si bien es cierto que estaba más vacía que antes, fue un placer volver a ver a Paco, Mar, Pilar, a los dos José Antonio y a José Manuel. Esa estación y la gente que allí trabaja me recuerdan el principio de una gran etapa de mi vida y siempre les tendré un cariño especial. Gracias.

La última de las estancias fue otra vez internacional, en esta ocasión en Bolonia, Italia, en el Instituto de Ciencias Atmosféricas y Clima. Fueron tres meses inolvidables, que darían fácilmente para escribir un libro, y que me cuesta mucho resumir en un párrafo. Gracias a Paolo Crisfanelli, Francescopiero Cazzolari y mi compañera de despacho, Maria Cristina, que no sólo me enseñaron cómo hacer ciencia de calidad, sino que hicieron de anfitriones y guías en un país y una ciudad con tantísimo que descubrir y disfrutar. Nunca olvidaré los paseos por el casco antiguo de Bolonia, los helados, las clases de italiano, las vistas desde el Monte Cimone y los viajes de un día en tren. Mil gracias por todo.

Una tesis es un proceso largo, que requiere esfuerzo y dedicación, y que involucra a muchísima gente. No hay suficientes palabras para mencionar y agradecer a todos los implicados sin caer en la repetición tediosa. Me limitaré a decir gracias, gracias de todo corazón a todos aquellos que os habéis encontrado un doctorando en vuestra vida, probablemente perdido y desorientado, y le hayáis dedicado palabras de ánimo y parte de vuestro tiempo. La investigación, aunque a veces pueda ser fatigante y angosta, también puede ser apasionante y muy gratificante cuando te acompaña gente como la que yo he tenido la suerte de encontrar. Gracias a todos.

Isidoro

Resumen

Según el Comité de las Naciones Unidas frente a las Radiaciones Ionizantes (UNSCEAR), el gas radón es responsable del 42% de la dosis de radiación total procedente de fuentes naturales. Su isotopo más común, ^{222}Rn, se emite desde materiales con alto contenido de radio, como es el caso del residuo fosfoyeso (FY), generado en la producción de ácido fosfórico. Este material contiene altas concentraciones de radio (unas 20 veces las de un suelo no contaminado), y es una fuente potencial de radón. A menos de 1 km de la ciudad de Huelva se encuentra un depósito de fosfoyeso de 1000 ha, área similar a la zona urbana. El objetivo de esta tesis doctoral ha sido desarrollar un método adecuado para la medida de exhalación de radón en fosfoyesos, y posteriormente analizar sus concentraciones en el aire atmosférico de Huelva.

En primer lugar, se estudió la exhalación de radón en fosfoyeso mediante dos cámaras de exhalación de referencia construidas con este material. El diseño permite cerrar la cámara y medir su exhalación sin modificar la capa emisora. Se estudió el rendimiento del método de medida de exhalación por acumulación en circuito cerrado y los ajustes lineal y exponencial a la curva de acumulación, utilizando diferentes equipos de medida y cámaras de acumulación. Aunque la aproximación lineal se emplea rutinariamente en la literatura, la constante de tiempo efectiva del sistema no siempre es adecuada para aplicar esta aproximación, subestimando significativamente la tasa de exhalación. Para extender la aplicabilidad del ajuste lineal se estudió la influencia del transporte lateral utilizando seis cámaras de acumulación cilíndricas que permitían aumentar la profundidad de inserción de la cámara en el suelo, demostrándose que la profundidad de inserción reduce la constante efectiva del sistema. Este resultado aumenta el intervalo de aplicabilidad del ajuste lineal, obteniendo medidas de exhalación fiables una vez que se ha alcanzado una profundidad de inserción de 6 cm. Estos resultados fueron verificados in situ con experimentos llevados a cabo en el depósito de fosfoyeso.

En segundo lugar, se midieron las concentraciones atmosféricas de radón en Huelva con dos estaciones de medida ubicadas a ambos lados del repositorio. La primera estación se instaló en el campus universitario de El Carmen, al norte del repositorio, y una segunda estación, La Rábida, ubicada al sur del repositorio. Las mediciones tomadas en la primera estación entre marzo de 2015 y marzo de 2016, se utilizaron para estudiar la evolución diaria del radón usando técnicas de clusterización. Se observaron curvas diarias típicas con variaciones estacionales, con máximos entre las 06:00 y 08:00 UTC (Tiempo Universal Coordinado) y mínimos alrededor del mediodía. Los valores medios estacionales oscilaron entre 5,6 y 10,9 Bq m^{-3} y los máximos entre 36,4 y 53,4 Bq m^{-3}. Se analizaron cuatro eventos utilizando medidas locales de variables meteorológicas y simulaciones atmosféricas mediante los modelos HYSPLIT (Hybrid Single Particle Lagrangian Integrated Trajectory) y WRF (Weather Research and Forecasting). Los resultados obtenidos indicaron que la contribución de fuentes de larga distancia puede tener un impacto significativo en los eventos radón alto. Las mediciones combinadas de las estaciones de La Rábida y El Carmen durante el año 2018 se utilizaron para estudiar el transporte local desde el repositorio. Se emplearon algoritmos de clusterización para identificar patrones diarios de radón, encontrando diferencias entre estaciones y una mayor ocurrencia de clústeres de radón alto en la estación de El Carmen. Las simulaciones atmosféricas con WRF se utilizaron como datos de entrada para el modelo de transporte lagrangiano FLEXPART (FLEXible TRAjectory Model). Este estudio sugirió que la estación de El Carmen se ve afectada principalmente por la difusión de radón desde el repositorio, mientras que el principal mecanismo de transporte en La Rábida es el transporte directo.

Abstract

According to United Nations Committee on Ionizing Radiation (UNSCEAR), radon gas is responsible for 42 % of the dose from natural radiation sources. The most common radon isotope, ^{222}Rn, is emitted from materials with a high radium content such as phosphogypsum (PG), a residue generated in the production of phosphoric acid. This material contains high concentrations of radium (about 20 times that of uncontaminated soil) and is a potential radon source. In the city of Huelva, a phosphogypsum repository with 1000 ha, similar to the city area, is located less than 1 km from the city. The objective of this doctoral thesis was to improve radon exhalation methods and analyze radon atmospheric concentrations in Huelva.

Firstly, to study radon exhalation from phosphogypsum, two reference exhalation chambers were made with a layer of this material. Its design allowed to close the box and measure its exhalation without perturbing the emitting layer. The performance of the closed-circuit accumulation chamber technique and the exponential and linear radon exhalation fitting methods was studied using different measurement devices and accumulation chambers. Although the linear approximation is routinely employed in the literature, the effective time constant of the measurement system is often not adequate to apply this approximation, leading to significative underestimations of the exhalation. To extend the applicability of the linear fit, the influence of lateral transport was studied using six cylindrical accumulation chambers that allowed to increase the insertion depth in the soil, showing that increasing the insertion depth effectively reduced the effective decay constant of the measurement system. This result increases the range of applicability of the linear fit, obtaining reliable exhalation measurements once a minimum insertion depth of 6 cm was used. These results were verified on measurements carried out on the phosphogypsum repository.

Secondly, radon atmospheric activity concentration was measured in Huelva at two stations located at both sides of the repository. The first station was installed on El Carmen university campus, to the north of the phosphogypsum piles the second station, La Rabida, is located to the south of the repository. Measurements taken on the first station between March 2015 and March 2016 were used to study the general radon daily behavior using clustering algorithms. Typical daily curves with seasonal variations were observed, with maximums between 06:00 and 08:00 UTC (Coordinated Universal Time) and minimums around noon. The mean seasonal values oscillated between 5.6 and 10.9 Bq m^{-3} and maximum ranged between 36.4 and 53.4 Bq m^{-3}. Four events were analyzed using local meteorology measurements and atmospheric modelling obtained with HYSPLIT (Hybrid Single Particle Lagrangian Integrated Trajectory) and WRF (Weather Research and Forecasting) models. These results suggested that contribution from long-distance sources may have a significant impact on high radon events in the area. The combined measurements of La Rabida and El Carmen stations during the year 2018 were used to study local transport from the repository. Hierarchical clustering identified daily radon patterns, finding differences between stations and a higher occurrence of high radon clusters in El Carmen station. Atmospheric WRF simulations were used as an input for lagrangian transport model FLEXPART (FLEXible TRAjectory Model). This study suggested that El Carmen station was influenced by radon diffusion from the repository while La Rabida station was only affected by direct radon transport.

Table of contents

List of Figures

List of Tables

1. Introduction

1.1 Overview and motivation

Throughout all its history, humanity has been exposed to ionizing radiation from natural sources. This reality was unknown until the final years of XIX century, when pioneers like Becquerel, Marie Curie and Rutherford started to investigate the radiation emitted by materials containing high concentrations from uranium and its daughters. Nowadays, it is proven that most of the radiation we all receive comes from natural radioactivity. It is also known that its main sources are cosmic radiation and natural radionuclides present in rocks and soils, even though its actual contribution depends on several factors such as altitude or local soils' composition (UNSCEAR, 2008).

All natural radionuclides are originated from uranium, thorium and potassium (Surkov and Fedoseyev, 1977), which can be considered the fathers of all natural radioactivity. Uranium and thorium are the initial elements of the three natural series, which begin with ^{238}U, ^{232}Th and ^{235}U isotopes (Figure 1). The nuclei of these long-lived unstable elements are the beginning of a decay chain that originates a significant portion of the natural radioactive elements present in rocks and soils. At ambient conditions, there is only one gaseous element ever present in these chains: radon. This gas is generated by radium alpha decay, being ^{222}Rn its most common isotope. The name radon usually refers specifically to ^{222}Rn isotope. Other relevant isotopes are thoron (^{220}Rn) or actinon (^{219}Rn), which are named depending on the decay chain where they originated.

Radon is a noble gas with atomic number 86. It is colorless, odorless and tasteless. Due to its electronic structure being complete, it has almost no chemical reactivity. Nevertheless, radon can be adsorbed in the structure of materials like charcoal or silica gel. Due to its gaseous nature and its long half-life (3.8 days) in relation to some atmospheric processes, it can be transported long distances through the lower layers of the troposphere. Once in the air, its concentration will not be altered due reactions with other air components but will be heavily modified by atmospheric constraints like convection or rainfall.

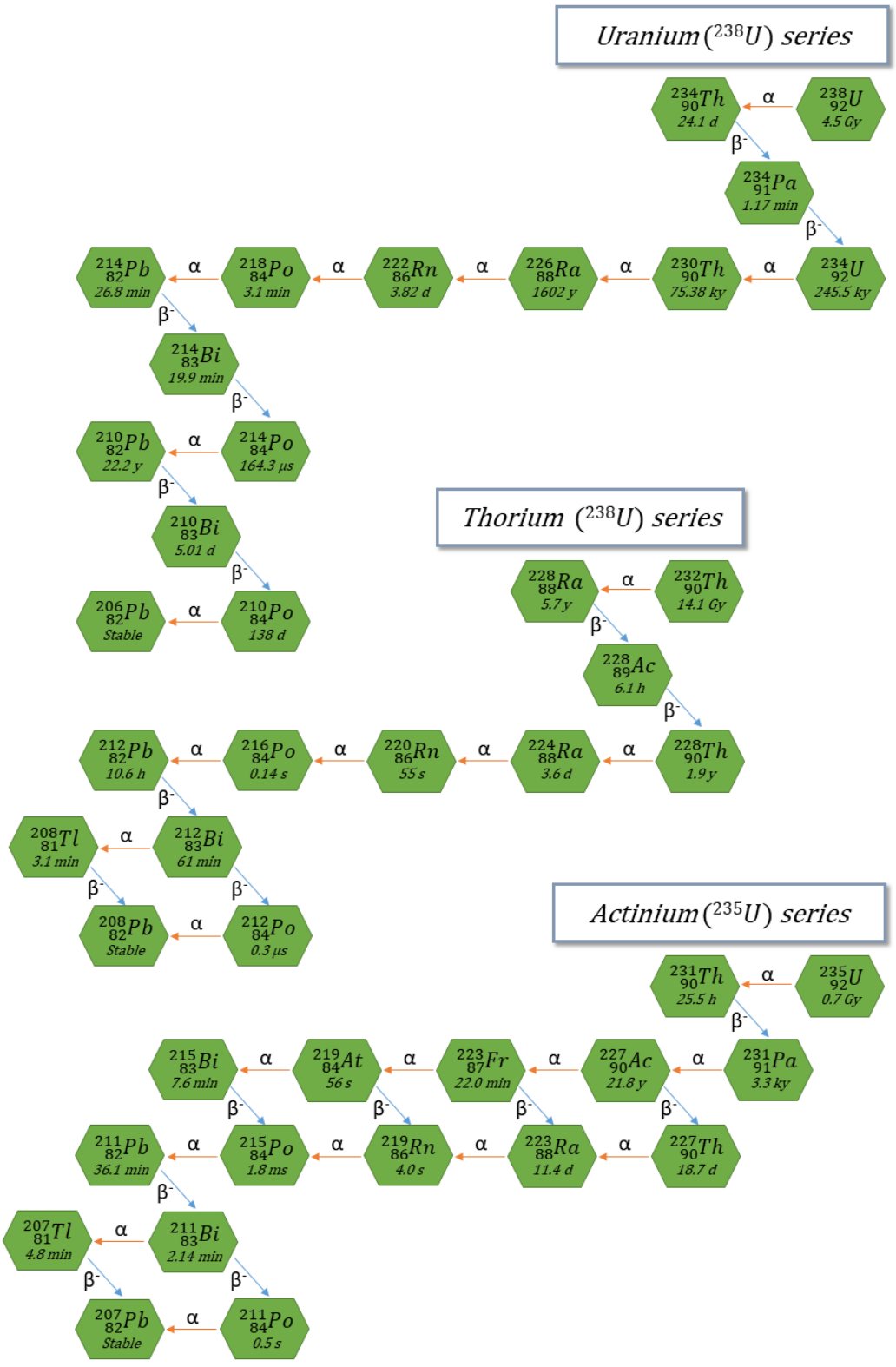

Figure 1. The ^{238}U, ^{232}Th and ^{235}U radioactive decay series.

Furthermore, radon is responsible for 42 % of the dose from all sources of natural radiation to the general population (Figure 2) (UNSCEAR, 2008). The most relevant radon isotope, ^{222}Rn, starts a disintegration chain followed by the decay of the so-called short-lived radon daughters: ^{218}Po (3 min), ^{214}Pb (27 min), ^{214}Bi (19.7 min), ^{214}Po (160 μs). Due the short half-life of its progeny, usually under 30 minutes, ^{222}Rn decay is followed by a fast cascade of alpha and beta radiation, ending in the long-lived daughter ^{210}Pb (22 years). Polonium, bismuth and lead are chemically active heavy metals that will form molecules in condensed phase and then attach to aerosol particles (Porstendörfer, 1994; Amgarou, 2003). When radon is breathed and decay within the respiratory system, these elements will deposit all its energy within the human body, significantly increasing the radiation dose that would have been received if the decay chain happened outside of the organism (James *et al.*, 1988; Darby *et al.*, 2005; Al-Zoughool and Krewski, 2009; Tchorz-Trzeciakiewicz and Kłos, 2017; Seo *et al.*, 2019). For this reason, the radiation dose due to radon is caused by its progeny rather than radon itself.

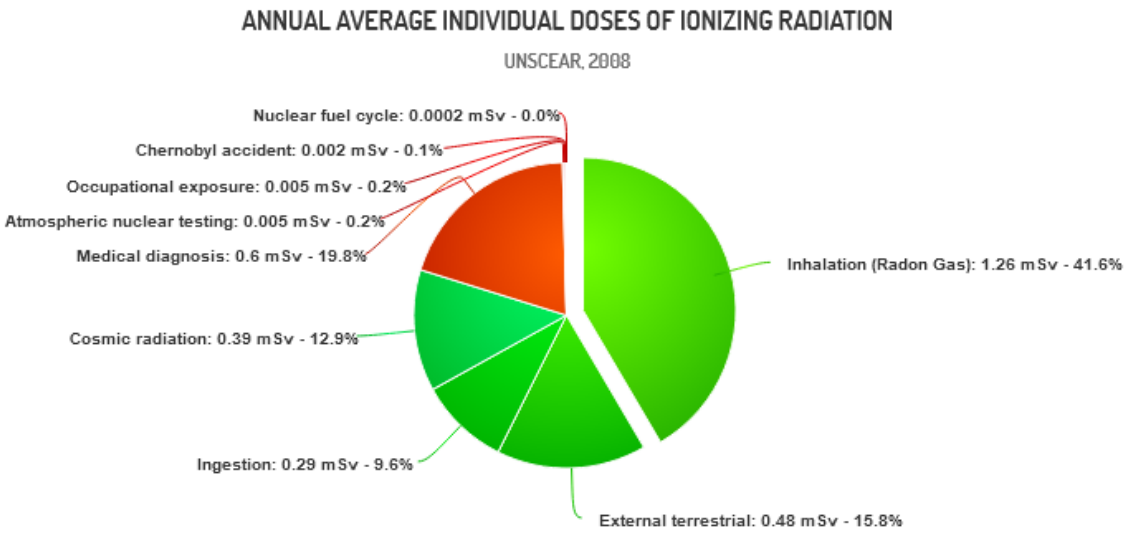

Figure 2. Annual average individual doses of ionizing radiation for natural sources (Green) and artificial sources (Red) (UNSCEAR, 2008).

However, the effective dose attributable to radon is a complex topic continuously under study worldwide (Planinić *et al.*, 1997; Porstendörfer, 2001; Vaupotič and Kobal, 2006; Xie *et al.*, 2014). Radon decay products are initially positively charged and quickly form clusters with air molecules and water vapour in what is called the unattached decay products, with an activity median aerodynamic diameter (AMAD) of less than 10 nm. Then, they might deposit on surfaces or attach to aerosols already present in the air, forming the attached decay products, within an AMAD range of 10-1000 nm. These fractions are important since different parts of the lungs are more susceptible to adsorbing particles within different AMAD ranges (ICRP, 1994b; Porstendörfer, 2001). Additionally, the quick interaction of radon daughters with the environment implies that radioactive equilibrium between radon and its short-lived daughters is almost never reached and has to be measured and modeled by an equilibrium factor.

Currently radon dosimetry is based on the study of the dose conversion factor (DCF), defined as the ratio between the weighted equivalent dose to the lung and the exposure to radon progeny. This factor can be obtained by either epidemiologic studies (ICRP, 1993, 1994c, 2010, 2015; Kreuzer *et al.*, 2015) or applying biokinetic and dosimetric models (Birchall and James, 1994; ICRP, 1994a,

2017; Vaupotič and Kobal, 2006; Leggett *et al.*, 2013). Both approaches heavily rely on the knowledge of radon concentrations, the equilibrium factor with its daughters, as well as the unattached and attached decay products fractions.

The aforementioned parameters vary substantially and have a significant impact on the effective radon dose to the general public. As an example, outdoors radon measurements average at 10 Bq m^{-3}, ranging between virtually 0 Bq m^{-3} for coastal regions to 100 Bq m^{-3} for sites with high radon exhalation areas in their surroundings. However, indoor radon reach concentrations as high as 85 000 Bq m^{-3}, measured in Sweden, with variable averages for different countries, e.g. 9 Bq m^{-3} in Egypt, 50 Bq m^{-3} in Germany, 86 Bq m^{-3} in Spain or 140 Bq m^{-3} for Czech Republic (UNSCEAR, 2000).

Besides the interest that radon has to public health, its general characteristics also make it suitable to be used in atmospheric sciences. Oceans have very low uranium or radium content, radon exhalation mainly occurs inland, and its low reactivity and half-life are perfect to identify high-radon air masses that have travelled for several days over land or low-radon air masses that comes from oceanic regions (Schery and Huang, 2004; Chambers *et al.*, 2011; Crawford *et al.*, 2013; Botha *et al.*, 2018). It is also an useful tool to validate atmospheric transport models, as its low reactivity implies that changes in its concentration can only be related to diffusion and convection processes alongside air masses (Jacob *et al.*, 1997; Hirao *et al.*, 2008; Arnold *et al.*, 2010).

Radon is also useful to analyze vertical mixing and the lower levels of the atmospheric boundary layer (ABL) structure (Moore, Poet and Martell, 1973; Chambers *et al.*, 2015; Crawford *et al.*, 2015; Podstawczyńska, 2016). Atmospheric stability has a significant influence on radon concentrations. During the day, the sun heats the soil and the air, creating an upwards air movement. This lower layer of atmospheric instability is called the convective mixed layer, and helps diluting radon in a vertical air column during daytime. At night, sun heating stops and the surface layer starts to cool down, generating a temperature inversion that creates a stable boundary layer (Figure 3). Under these conditions, newly generated radon is forced to stay within the recently created surface layer. Thus, stable conditions will help to accumulate radon in the lower layers of the atmosphere.

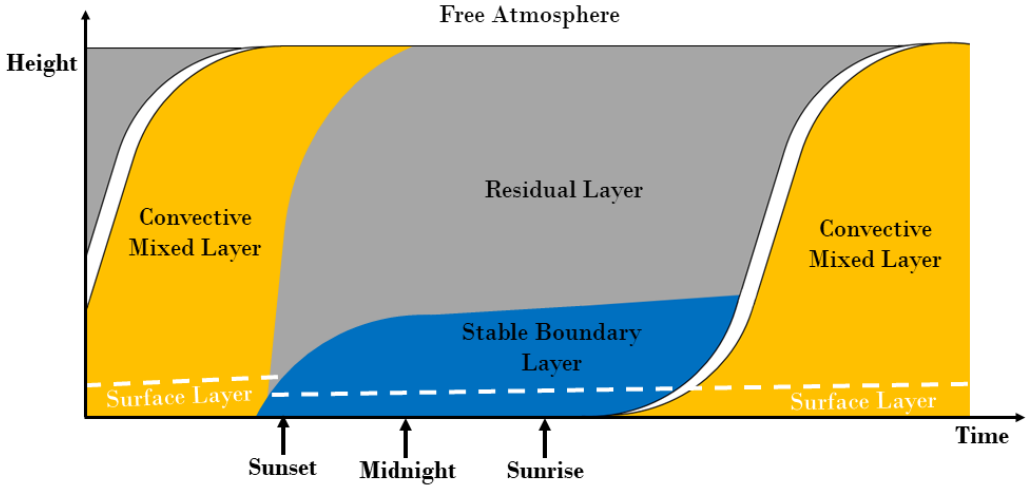

Figure 3. Idealized scheme of the Atmospheric Boundary Layer daily evolution.

In order to enter the atmosphere or the interior of dwellings, radon has to cross the surface of the soil, walls or building materials and reach the surrounding air in a process typically called radon exhalation. However, not all radon present in soils or building materials will exhale into the

atmosphere. Radon that generates inside the grains have to reach the pore space in the material by alpha recoil or diffusion within the grains. This process is called radon emanation. Since radon mobility inside the grains is extremely low, the main transport process will be alpha recoil. (Nazaroff, 1992). Radon recoil range depends on density and composition of the material, being 34 nm quartz, 77 nm in water and 53 um in air (Sakoda, Ishimori and Yamaoka, 2011). As such, radon needs to be generated close to the surface of the grains but not as close to impact another grain and get stuck. Once in the pore space, radon may reach the surface, transported through the material by diffusion or convection processes.

Radon exhalation measurements have been a relevant topic of research in the literature (Jonassen, 1983; Butterweck-Dempewolf and Schuler, 1996; Quindós *et al.*, 2002; Grossi, Vargas and Arnold, 2008; López-Coto *et al.*, 2009; Sahoo and Mayya, 2010; Hosoda *et al.*, 2011; IAEA, 2013; Abo-Elmagd, 2014). This is due to the complexity of the emanation and exhalation mechanisms, that depends on factors like diffusion, humidity, or pressure gradients. High humidity in the material will increase the presence of water in the pore space, reducing the diffusion capacity within the pores as water has a higher stopping power than air. Depending on the specific properties of the material, radon exhalation increases quickly until a maximum is reached between 0 to 10 % water content, and diminishing as moisture is further increased (Hosoda *et al.*, 2007; Faheem and Matiullah, 2008). This effect can have a significant influence during dry or wet periods, depending on local precipitations (Müllerová *et al.*, 2018). Although typical temperature variations do not have a significant impact on emanation or exhalation (Porstendörfer, 1994), strong pressure gradients will significantly increase convection movements through the pore space, enhancing radon exhalation (Redeker, Baird and Teh, 2015; Yarmoshenko *et al.*, 2018).

When considering radon exhalation there are a number of factors to consider, such as the radium content or the radon diffusion length, which measures the capacity of radon to travel across the material before decaying. This parameter is critical, as most materials will have diffusion lengths less than 1 m, e.g. 1 m in gypsum, 0.4 m in limestone or 0.006 m in granites (Keller and Hoffmann, 2000), implying that only the last meters or even millimeters of material may account for all radon exhaled to the atmosphere. This is especially important in NORM repositories, as radon diffusion length advises in favor of stockpiling in height rather than in length. Exhalation rates can vary substantially based on all of this factors, from almost 0 to non-uranium rich soils to 36 kBq m^{-2} h^{-1} found on an uranium waste repository (Kumar, Sengupta and Prasad, 2003; Sahoo *et al.*, 2010; Bollhöfer and Doering, 2016).

Thus, exposure to radon will largely depend on local meteorological conditions such as precipitations, pressure differences or local wind speeds, and radon exhaled by soils and building materials, which will be subject to the proximity to uranium-rich or radium-rich materials, either natural or manmade. Granitic and high degree metamorphic rocks derived from sedimentary limestone or phosphate rocks are some examples of rocks with high radon content (Suarez Mahou *et al.*, 2000). Special attention has to be paid to activities related to Naturally Occurring Radioactive Materials (NORM), such as metal and coal mining, phosphate industries or oil and gas drillings, among others (UNSCEAR, 2008).

As an example of these industries, in the city of Huelva, the phosphate industry was active during almost 45 years, producing large quantities of phosphogypsum (PG). This material, has a radium content of approximately $650 \pm 50\ Bq\ kg^{-1}$, higher than the average radium activity concentrations in Spanish soils, 32 Bq kg^{-1} (Quindós *et al.*, 1994), hence being a potential source of radon in the environment (Bolívar, García-Tenorio and García-León, 1996b). PG was stacked in four different

zones during the production period at a rate of $2.5 \cdot 10^6\ tons/year$, covering a $1000\ ha$ area located in Tinto River estuary, less than 1 km from the city (Figure 4). The zone 1 covers an extension of 450 ha, accumulating approximately $25 \cdot 10^9\ kg$ of PG and other urban and mining wastes. Rehabilitation of this area was finished in 1992, 30 cm of soil cover with vegetal cover were added and several tenths of 1.5 m soils hills were built in the area. Zone 2 comprehends 270 ha of uncovered PG, reaching 25 m of height in some areas. The zone 3, with 180 ha, have not been used for PG disposal since 1992. Lastly, zone 4 (130 ha), started its rehabilitation works in 1998. Since zones 2 and 3 are still uncovered, radon levels nearby the PG repository could be enhanced by its presence.

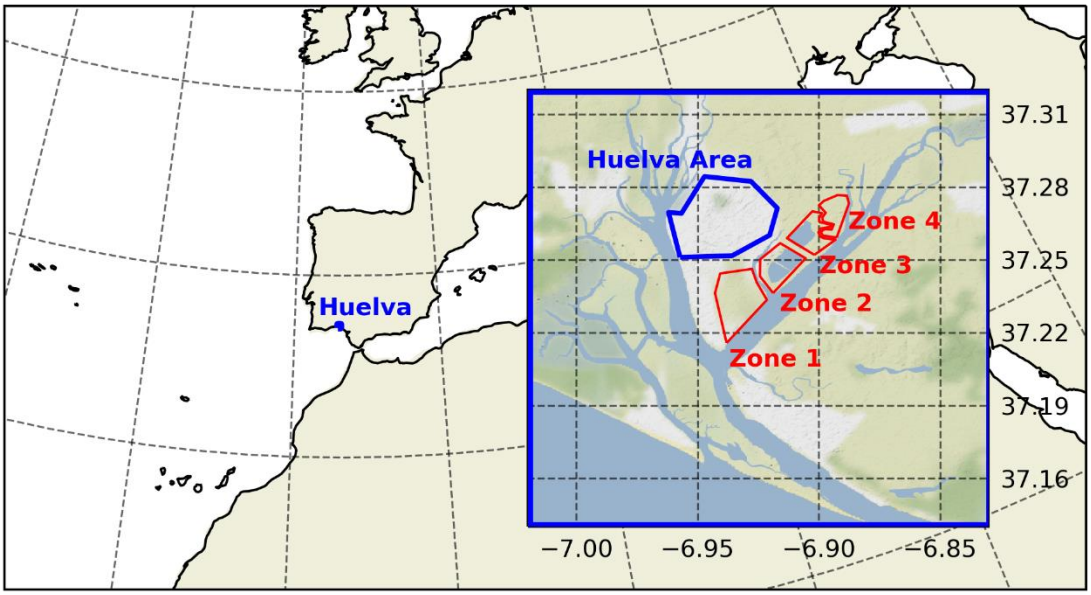

Figure 4. Location of Huelva city and the phosphogypsum piles.

The city of Huelva (Figure 4) is a perfect location to study radon behavior as it combines a potential local source, due to the PG repository, with a mix of atmospheric regimes that bring oceanic and continental air masses to the area. Synoptically, most of the air masses have an Atlantic Ocean influence, with more than a 50 % relative frequency throughout the year. Air masses from the Artic region have a maximum 20 % frequency in November, being above 10 % during cold months (Oct-Feb), as expected. Mediterranean Air masses are more common between May and November, with relative frequencies between 12 and 25 %. Continental air masses coming from Europe range between 10 and 20 % relative frequency, being more common in spring (Mar-May) (Toledano *et al.*, 2009).

Being a coastal site, the local mesoscale regime is greatly influenced by sea-land breezes. The occurrence for these breeze patterns is above 30 % from May to September, reaching its maximum in July and August. Two breeze patterns were identified in the area: pure breeze and non-pure breeze (Adame, Bolívar, *et al.*, 2010; Adame, Serrano, *et al.*, 2010). The pure breeze consists of a midday flow from SW, perpendicular to the coast, with an average speed between 2 and 3 m s^{-1}. The sea breeze ends around 20 UTC, transitioning clockwise from SW to NE, maintaining this direction during the night, from 03 to 08 UTC, with wind speeds around 2 m s^{-1}. Afterwards, the wind turns clockwise again to SW direction. The non-pure breeze has a similar behavior during midday, but instead transitions to a NW direction during the night, instead of NE, and rotates counterclockwise instead when shifting from the land to the sea breeze. Non-pure breeze is also characterized by higher wind speeds than its counterpart.

Due to the special location and circumstances related to the city of Huelva, extensive research about the PG piles have been done in past two decades. Being a NORM material, the phosphogypsum in the repository helped understanding natural radioactivity and its effects in the surrounding soils and salt-marshes and to public health (Bolívar, García-Tenorio and García-León, 1995, 1996a, 1996b; Bolívar *et al.*, 2009; Pérez-López *et al.*, 2010). The restoration efforts made on zones 1 and 4, and the future plans to restore zones 2 and 3, have impulsed a better understanding on soil remediation techniques and their efficiency to inhibit radon escape to the atmosphere (Mas *et al.*, 2006; Dueñas *et al.*, 2007; López-Coto, 2011). There are some relevant works regarding radon exhalation, studying both radon exhalation measurement systems and exhalation variability on the PG piles (López-Coto *et al.*, 2009, 2014), as well as investigating atmospheric radon behavior in the area (Grossi *et al.*, 2012, 2016; Hernández-Ceballos *et al.*, 2015; Vargas *et al.*, 2015).

The FRyMA (Radiation Physics and Environment) research group, which belongs to the Department of Integrated Sciences of the University of Huelva, installed two atmospheric radon monitors in the area. The first one was installed on 2014, alongside the atmospheric measurement station already installed by the group on the roof of El Carmen university campus, inside the city of Huelva. The second radon monitoring station was installed on 2017 on the university campus of La Rabida, which is located on the other side of the PG piles and the Tinto river. The combination of the two measurement stations, located at opposing sides of the repository, offers a unique opportunity to further study radon transport in a coastal area like Huelva, affected by complex mesoscale and synoptic atmospheric processes.

These radon measurement stations could be coupled with exhalation measurements over the repository to study radon concentrations in the area, providing insightful information about radon behavior in both soil and atmosphere. In order to achieve this, it is necessary to understand the exhalation measurement procedure, taking into account specific elements due to the special conditions occurring in the PG repository, such as its high humidity and salinity, its radium content or wind regimes that may affect not only the natural exhalation but the measurement procedure itself. To account for possible interferences in the measurement process, a reference exhalation chamber was built with PG from the piles, aiming to reproduce an exhalation soil under controlled conditions and allowing to further study the exhalation process and how to measure it with accuracy.

This thesis was developed under the MINECO project "Fluxes of radionuclides emitted by the PG piles located at Huelva; assessment of the dispersion, radiological risks and remediation proposals" (Ref: CTM2015-68628-R). One of the goals of this project is to evaluate radionuclides fluxes from the PG piles to the atmosphere. To achieve this, there are two possible ways: i) Measure the radon exhalation rate on the repository, including both its special and temporal variability, or ii) simulate its behavior with atmospheric transport models and compare their results with the atmospheric radon measurements taken in the area. Both options were pursued during this thesis.

1.2 Objectives and milestones

Taking into account the commented previous problems, this work has the main goal of ***investigating the phosphogypsum stacks influence on the radon concentration in the surroundings of the city of Huelva.*** In order to achieve this objective, it is necessary to investigate both the atmospheric radon concentration and the radon sources, i.e. the exhalation rate of the PG piles.

As stated previously, the study of exhalation rates is a complex topic, thus requiring the definition of a second objective, which consists on ***verify and improve the performance of the exhalation***

measurement systems currently employed and apply them to study the exhalation rate of phosphogypsum.

On one hand, the first objective can be further described in the following specific objectives:

Identification of meteorological conditions that enhances radon concentrations in Huelva city.

The instrumentation of the FRYMA research group at Huelva University was used to measure radon concentrations in the area of study. Hourly radon concentrations were measured at El Carmen University Campus from 2014 until 2019, while at La Rabida station measurements were made from 2017 to 2019. El Carmen data was firstly used to test clustering techniques on hourly radon concentrations. This allowed to gain some insights about the radon behavior in the area and its relation to other meteorological variables, such as temperature, pressure, relative humidity or the height of the ABL.

Study of long-range radon transport processes affecting the city of Huelva

The measurement station in El Carmen was installed in 2014 and worked as the only radon station from 2014 to 2017. This first set of radon measurements was used in combination with local meteorology information, clustering techniques and back-trajectory models. This approach allowed to investigate long-range radon transport processes and its possible influence on local radon concentrations.

Application of two measurement stations to identify local transport and differences in radon levels

A second measurement station in La Rabida university campus was installed in 2017 to study differences of local radon transport due to the PG repository in detail. The previously acquired knowledge, i.e. influence of local meteorology on radon behavior, clustering techniques and modelization, was employed again to describe radon concentrations measured on both stations simultaneously.

On the other hand, the second objective will be divided in specific milestones as follows:

Creation of a reference exhalation soil.

With the aim of comparing different measurement approaches, it is necessary to use a material with a constant and reliable exhalation rate. This material needs to be measured with precision and accuracy, ensuring that its exhalation can be measured with different approaches. In this work, two reference exhalation boxes were made out of polypropylene, using phosphogypsum as the source material producing radon. These boxes were designed to allow the accumulation of radon inside without disturbing the PG itself, thus providing a way to measure radon exhalation systematically. This system also allows to use different measurement techniques on the layer of PG that can be verified afterwards comparing them to the reference measurements.

Comparative and calibration of different measurement setups.

Once finished, the reference exhalation boxes will be used to compare different measurement setups, including combinations of measurement devices and accumulation chambers. Several radon measurement instruments were employed: two Alphaguards, one Rad 7 and one Radon Scout, which will be described on future sections. These measurement devices were used alongside several accumulation chambers with different volumes and areas. These tests will allow to gain some

experience about the measurement techniques on controlled conditions, learn the best-practices and find the measurement setup that works best on different conditions.

Design of a measurement system to allow continuous measurements on the PG stacks.

The information achieved will be used to design a measurement system capable of measuring radon exhalation in a continuous way. This will be a great help to study seasonal or even daily variations in radon exhalation. Moreover, it could help to explain atmospheric radon concentrations in the area of study, as it will provide with the information needed to characterize the PG stacks as a radon source in atmosphere models.

1.3 Outline

This manuscript is organized in four chapters. The first section has offered an introduction on the topic of the thesis, providing some useful background to the reader. A description of the state of the art in the topic of atmospheric radon and its exhalation has been included, as well as a description of the area of study and its special circumstances. It also has presented the main goals and milestones that the thesis aims to fulfil, including a short description of the steps followed to achieve them.

The second part describes in detail the methodology used during this research. Firstly, the techniques employed in the literature to measure radon concentration are presented. A short description of some measurement devices is also included. Secondly, a detailed description of how to measure radon exhalation is provided. It includes the complete theoretical deduction of the governing equation of the radon transport process across the soil up to the surface of exhalation. Thirdly, there is a complete description on how the reference exhalation surface was designed and built, including how its exhalation rate was verified and monitorized. Afterwards, a detailed depiction on the atmospheric measurement station used to measure radon is given. Finally, there is a description on the software employed to carry out this work.

Chapters three to six comprehends the results and its discussion. It consists of the published scientific papers as they appear in their respective journals. The first two papers focus on the radon exhalation measurements, the development of the reference exhalation boxes and some insights on how to improve the reproducibility of the exhalation measurements by inserting the accumulator inside the soil. The second two papers describe the atmospheric radon behavior in the city of Huelva, the clustering techniques employed to study radon concentrations and the influence of long-range and local transport on radon levels in the city of Huelva.

Finally, chapter four consists of a summary of the conclusions obtained thanks to the preceding works. It aims to be a general conclusions section that highlights the main results of this work. Additionally, future lines of research are included and discussed briefly. A complete list of all references used in this work is appended at the end of this section.

2. Materials and methods

As explained in the outline, this chapter includes a description of the measurement techniques, devices and software tools employed during this thesis. First, the main alpha particles measurement principles are examined. Secondly, the measurement devices employed during this thesis are mentioned and described briefly. Special emphasis was taken with the ARMON system, as it was heavily adapted to work almost autonomously. Subsection three consists on a thorough explanation on how radon exhalation were taken. The fourth subsection contains information about the meteorological datasets and simulations models employed. Finally, subsection five contains a description on the software developed to manage and study all the data collected during the thesis.

2.1 Measurement of radon concentrations

As described in the introduction, radon is measured using the alpha decay of its daughters, either by direct or indirect methods. There are several alpha emissions between ^{222}Rn and the stable ^{206}Pb that can be used to measure Rn concentration (Figure. 1). The most used are the immediate ^{222}Rn alpha decay progeny, i.e. ^{218}Po and ^{214}Po, or a combination of them. Usually, the measurement method involves a container or chamber which is placed exposed to the air to be measured or over the surface of interest. Then, the radon concentration in the chamber is measured by registering the alpha events caused by radon or its progeny.

It is important to consider the difference between measuring thoron (^{220}Rn) and radon (^{222}Rn) since both isotopes will decay by emitting alpha particles. In environments where thoron concentrations are significant it is important to remove it before measuring or use a device capable of performing alpha spectroscopy, allowing to distinguish the concentrations of both elements.

Moreover, radon and its daughters are never found in equilibrium in ambient conditions. For this reason, it is important to remove radon progeny before sampling, ensuring that the progeny present in the device is only due to radon decay inside the measurement chamber. Radon decay products are not chemically inert and will react with other elements or stick to aerosols. For this reason, the most common way to remove radon progeny is to place a filter before the sampling system to eliminate particulate activity. Since radon is inert, it will not be trapped in the filter. This allows to measure on one side radon progeny, measuring its activity with the filter, and radon gas, measuring the newly generated radon daughters after the filtration.

The reactivity of radon daughters is especially problematic in the case of ^{210}Po, as this element has a half-life of 138 days, much longer than its predecessors. This can generate an accumulation of ^{210}Po in the detection device, increasing the alpha activity in the measurement chamber and generating noise. Those devices capable of doing alpha spectroscopy can distinguish its energy and neglect its influence but if that is not the case, the device can be rendered useless if ^{210}Po counts are too high and its influence cannot be detracted.

2.1.1 Basics of alpha particles detectors

Ionization chambers

The working principle of ionization chambers is based on the capacity of alpha particles to ionize some gas, like air itself, while dissipating its energy. Essentially, they are a ionization detector working on the proportional counting region (Knoll, 2010). Usually, the ionization chamber is a cylinder with a built-in central collection anode. Using an electric field, the ionization products are driven to the anode and measured as an ion current. Radon is measured by means of the current, which is proportional to the energy of the alpha particles emitted. Thus, ionization chambers are capable of performing alpha spectroscopy and distinguish the energies of the different radon daughters. The efficiency of ionization chambers will depend on the gas stored inside the chamber, as its density and composition will have an impact on how frequently ion pairs are generated and detected.

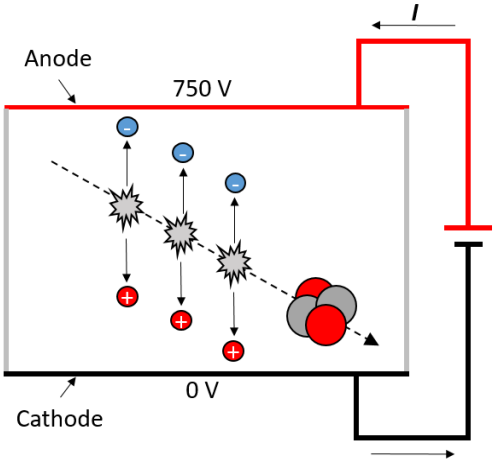

Figure 5. Scheme of an ionization chamber.

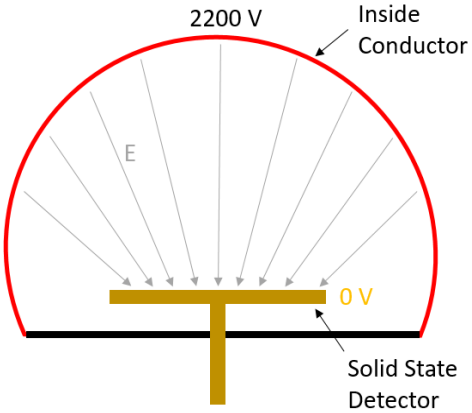

Figure 6. Scheme of a solid state detector.

Solid state detectors

Use of solid state detectors rely on using an electric field to collect recently generated and positively charged radon daughters, usually ^{218}Po and ^{214}Po, on the flat surface of a semiconductor detector. Once the trapped particle disintegrates on the surface of the detector, there is a 50 % chance that the emitted alpha particle is collected on the detector instead of going back to the chamber space. The collected alpha particle produces free electrons and holes in the semiconductor material that are directed by an electric field to the electrodes (Knoll, 2010). The number of electron-hole pairs is proportional to the energy of the alpha particle, allowing to perform alpha spectroscopy and distinguish between radon and its progeny.

Although this technology is more complex, semiconductor detectors generally have more resolution than ionization chambers. The energy required to produce the electron-hole pair is lower than the required to ionize the air, resulting in a higher energy resolution. Moreover, electrons move faster, ensuring a higher time resolution. Finally, due to its density, solid state detectors require less material as alpha particles will rapidly deposit its energy inside the semiconductor, compared to a gas detector.

Scintillation Cell

Scintillation cells are based on scintillation materials that generate light photons when interacting with ionizing particles (Knoll, 2010). Some examples are cesium iodide (CsI), sodium iodide (NaI) or zinc sulphide (ZnS). When these materials are exposed to incident radiation, it generates photons

that are collected onto a photomultiplier that detects and amplifies its signal. This signal is then measured by an electronic device and converted to electric pulses that are proportional to the energy deposited by the ionizing particle, allowing to perform alpha spectroscopy and detect radon. In general, as in semiconductor detectors, the solid nature of scintillator materials allows them to have higher energy resolution than ionization chambers.

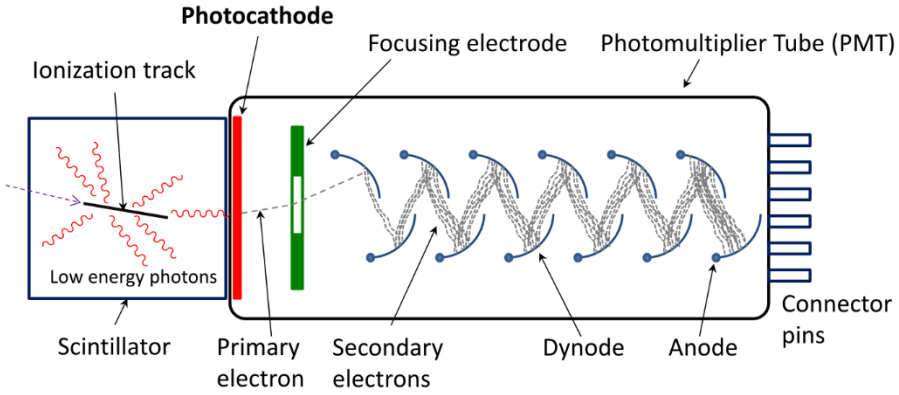

Figure 7. Scheme of a scintillation cell

Electrets

An electret is a passive radon detector similar to an ionization chamber (Kotrappa *et al.*, 1990; Kotrappa, 2015). The electrical field is provided by an electrically charged Teflon disc, which also serves as a detector. The ionization produced by alpha decay inside the chamber is collected by the electrical field and guided to the detector, decreasing the initial charge of the electret. The voltage drop over the measurement period can be used as a measure of the average radon concentration in the chamber.

The efficiency and resolution of the detector are similar to an air-filled ionization chamber, but also depends on the electret material used and its initial charge. This technique is usually employed to perform averaged long-term measurement over several months.

Activated Charcoal

Radon concentration measurement by activated charcoal relies on the adsorption of radon atoms on the surface of charcoal (Spehr and Johnston, 1983; Gómez *et al.*, 1991; Iimoto *et al.*, 2008; Alharbi and Akber, 2014; Tsapalov, Kovler and Miklyaev, 2016). This method requires that the charcoal is purged and placed on a hermetically closed canister before being exposed to the air to be measured. After the measurement period, the canister is closed hermetically again and measured after the radon progeny has reached equilibrium. The activity of the canister can be measured in a previously calibrated gamma spectroscopy device using the gamma emissions of radon daughters. This technique can provide reliable measurements but requires careful handling of the canisters and knowledge of the half-time periods involved to perform correct and accurate measurements.

Since charcoal is also prone to water adsorption, it also requires that the water content before and after the measurement is taken into account, making them less appropriate to measure for humid environments.

2.1.2 Measurement devices

Alphaguard

The Alphaguard is a portable real-time radon measurement device developed by Bertin Instruments. It is based on the ionization chamber technique and allows to measure a wide range of radon concentrations, from 2 to $2 \cdot 10^6$ Bq m^{-3}, being capable of performing alpha-spectroscopy due to its pulse-counting ionization chamber. Its sensitivity is the highest of all measurement devices used in this work: 5 cpm at 100Bq m^{-3}.

Its ionization chamber consists of a cylindrical volume of 0.56 L. Alongside its longitudinal axis there is a central electrode that is on a potential of 0 V while the interior outer surface is charged up to 750 V. The center electrode collects the ionization products generated by radon daughters, ^{218}Po and ^{214}Po, and processes the signal by a digital signal processing unit that computes the radon concentration (Bertin Technologies, 2019).

Alongside radon concentration, the system measures temperature, pressure and relative humidity. The Alphaguard includes an inbuilt quality assurance system to ensure the validity of the measurements. Additionally, its calibration its traceable to different national standards (PTB, NIST, NPL). Despite its mentioned advantages, it is sensible to ^{210}Pb contamination.

Rad 7

Rad 7 is a versatile real-time radon and thoron detector built by DURRIDGE Company, Inc. The principle of measurement is based on a solid state detector, capable of doing alpha spectroscopy. Its internal cell is a semi-sphere of 0.7 L covered by an electrical conductor charged up to 2.5 kV that leads the radon progeny onto a Passivated Implanted Planar Silicon (PIPS) placed at the centre of the semi-sphere.

The device allows to compute the radon concentration with both radon daughters, ^{218}Po and ^{214}Po, or, alternatively, only the short-lived ^{218}Po (SNIFF Mode). This makes the device capable of measuring fast radon variations with precision, as the first radon daughter concentration will follow the concentration of its parent. Since the Rad 7 measures alpha decay directly, it is immune to ^{210}Pb contamination. Its sensibility is 1.3 cpm at 100 Bq m^{-3} for normal mode and 0.67 cpm at 100 Bq m^{-3} for sniff mode.

Radon Scout

The Radon Scout gas diffusion detector based on a silicon detector developed by SARAD GmbH. It is an easy to use device that can be employed almost anywhere due its small size and the absence of moving mechanical parts. It allows the measurement of temperature, relative humidity and pressure and is powered directly by batteries. It is an integrating device based on a solid state detector with a configurable measurement period and a sensitivity of 0.18 cpm at 100 Bq m^{-3}.

Atmospheric Radon MONitor (ARMON)

The ARMON system was designed at the radon laboratory (LER) of the Institut de Tècniques Energètiques (INTE) of the Universitat Politècnica de Catanlunya (UPC) (Grossi *et al.*, 2012). The monitor is based on alpha spectroscopy performed by a Passivated Implanted Planar Silicon (PIPS) detector.

The system consists of a 20 L sphere with a PIPS detector on its top. The ^{222}Rn concentration of the sampled air is continuously monitored within the volume of the sphere. Radon is estimated using the α-activity of ^{218}Po collected on the PIPS detector by an 8 kV potential electrostatic field.

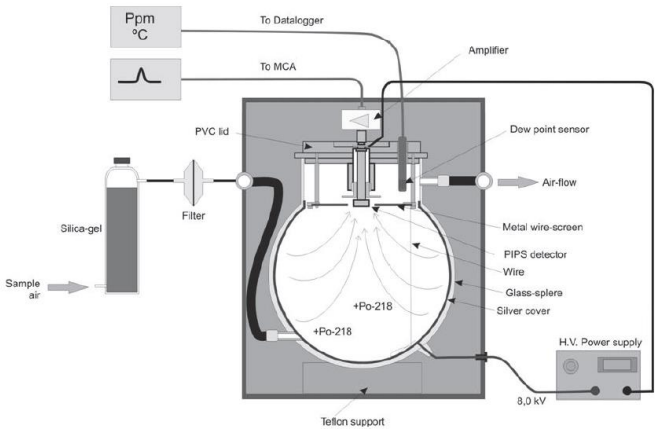

Figure 8. Scheme of the ARMON device

This device requires very low water content in the interior air to not neutralize the alpha particles and reach the PIPS detector surface. Thus, an external support system must be employed to control humidity, flow and to perform the alpha spectroscopy from the alpha counts and calculate the radon concentration. The previously cited adaptation to work autonomously is further described in subsection 2.4.

2.2 Radon Exhalation

2.2.1 Fundaments

Radon concentrations in soils and building materials are 3-4 orders of magnitude higher than gas concentrations in the atmosphere, generating a great concentration gradient between radon-generating soils/materials and ambient air (Porstendörfer, 1994). As long as the radon generation by the decay chain of 238U continues, this gradient will be maintained. The process by which radon escapes the emitting material across a defined area and reach the atmosphere is called radon exhalation ($Bq\ m^{-2}h^{-1}$).

Once radon decay happens inside the grains of the material, the newborn radon atom can be propelled to the pores by alpha recoil or, if it is close enough the grain surface, escape by diffusion within the grain. Once in the porous space, a portion of radon can travel towards the surface, by convection and/or diffusion processes, contributing to the exhalation. The exhalation process depends upon several factors, such as:

- Emanation factor.
- Effective porosity.
- Diffusion coefficient ($m^2\ s^{-1}$).
- Humidity content.
- Radium concentration ($Bq\ kg^{-1}$).

On one hand, the emanation factor is defined by the fraction of radon atoms that successfully escape the grains and reach the pore space. Alpha recoil and diffusion are the two components of this process but, due to the low diffusion coefficient of radon gas in solid materials, alpha recoil is assumed to be the main emanation pathway. Depending on the type of material, radon recoil is in the range of tenths of nanometers, 10^{-8} m, while radon diffusion length is between 10^{-13} and 10^{-32} m, significantly lower than alpha recoil (Sakoda, Ishimori and Yamaoka, 2011).

On the other hand, the effective porosity measures how connected the pores are within the material. Soils with high porosity facilitates gas movement in the pore spaces, allowing more radon atoms to reach the surface. As radon diffuses through the pore space in the material, it will travel from

higher to lower radon concentrations areas, creating a radon gradient from the deeper areas of the soil, where there is more radon, to the air at the surface of the material, where the radon content is much lower. This molecular diffusion process is characterized by the diffusion coefficient, which is described by Fick's first law and characterizes the rate of radon movement through the soil. Convective processes such as pressure differences or wind on the surface of the soil will be enhanced as well by a higher effective porosity, allowing radon to be transported easily through the pore space by the pressure gradient.

Emanation, porosity, diffusion and convection are greatly influenced by moisture content. The alpha recoil stopping distance in water is lower than in air, allowing the radon atoms to be decelerated before incrusting themselves in another grain. However, if the pore space is filled with water, radon diffusion and convection processes could be severely restricted, reducing its migration distance across the soil. Depending on the soil, two types of emanation relation with moisture content have been reported (Figure 9). The first kind shows an increase from no water content until a saturated value is reached, staying constant after a certain moisture content. The second type present a quick increase between 0 and 10 % of humidity, reaching and maximum, and decreasing afterwards as the water content in the pore space increases.

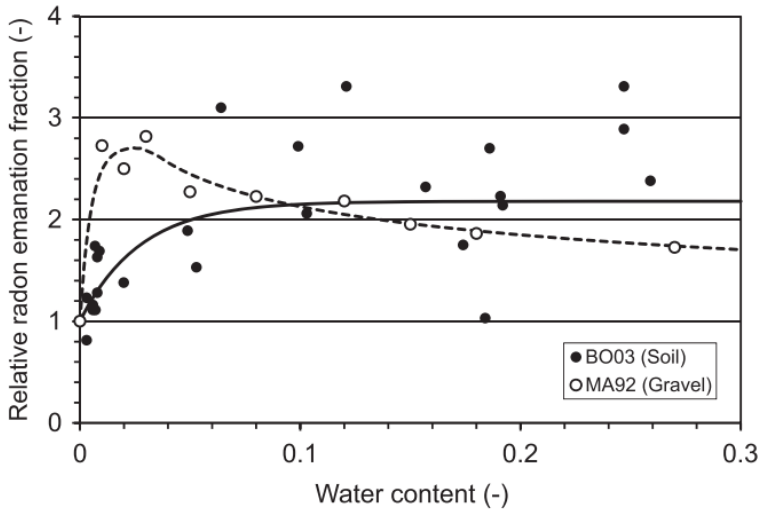

Figure 9. Relative radon emanation fraction as a function of water content *(Sakoda, Ishimori and Yamaoka, 2011).*

Finally, radon emanation will be characterized as well by the radium content of the material, as this element is responsible of radon generation by alpha decay. Those materials with higher radium content will have more radon atoms available to escape the grains, travel through the pores by diffusion and reach the surface, flowing into the atmosphere by exhalation. In summary, radon emanation and its transport through the material is a truly intricate topic that would deserve several thesis and review articles on its own. More information can be found in the literature (Spehr and Johnston, 1983; Nazaroff, 1992; Chao and Tung, 1999; Sasaki, Gunji and Okuda, 2004; Sakoda, Ishimori and Yamaoka, 2011; Ryzhakova, 2012).

Deduction of the theoretical expression for radon transport within the material

To measure the radon exhalation, it is necessary to deduce the rate at which it escapes through the soil-air interface, but first we need to know how radon behaves within the soil. Let us consider a soil matrix with a continuous radon generation within its grains and an air-soil interface, as depicted in

Figure 10. Radon concentration, C_{Rn}, transport equation in the soil will follow the general convection-diffusion equation:

$$\frac{\partial C_{Rn}}{\partial t} = \nabla \cdot (D_B \nabla C_{Rn}) - \nabla \cdot (\vec{v}_d \, C_{Rn}) + S - R \tag{1}$$

Where D_B is the radon diffusion coefficient, $\vec{v}_d$ is the convective flow rate in the material, and S and R are the radon source and removal terms, respectively. In general, convection effects are usually neglected, assuming consistent convective flows do not exist or are spurious in nature. Consequently, molecular diffusion is considered to be the dominant term, neglecting convection influences. (Nazaroff, 1992; Porstendörfer, 1994; Mayya, 2004; López-Coto *et al.*, 2009; IAEA, 2013; Onishchenko, Zhukovsky and Bastrikov, 2015). Conversely, special care must be taken as this assumption cannot be considered to be always true for buildings, since its special circumstances may enhance consistent airflows and inhibit diffusion from the soil (Nazaroff, 1992).

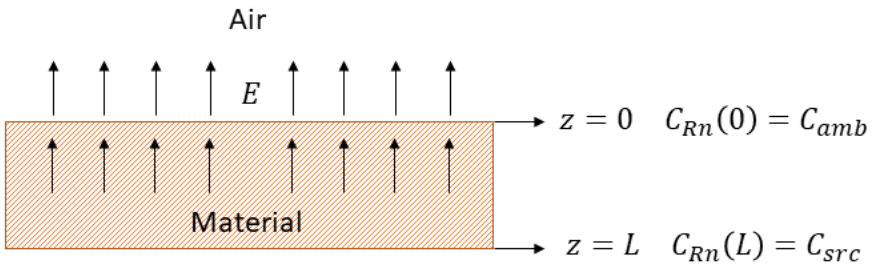

Figure 10. Scheme of the air-material cross-section.

In the case of uncovered soils, it is accepted to consider diffusion transport to be the only relevant transport process. Thus, for one dimensional transport across the z axis in a homogeneous and isotropic material, the steady-state transport equation can be now rewritten as:

$$D_B \frac{\partial^2 C_{Rn}}{\partial z^2} + S - R = 0$$

$$\frac{\partial^2 C_{Rn}}{\partial z^2} + \frac{\lambda_{Rn}}{D_B} C_{src} - \frac{\lambda_{Rn}}{D_B} C_{Rn} = 0 \tag{2}$$

Where:

- C_{Rn} Radon concentration ($Bq\ m^{-3}$).
- z Vertical position in the material (m).
- λ_{Rn} Radon decay constant (s^{-1}).
- D_B Diffusion coefficient ($m^2 s^{-1}$).
- C_{src} Radon source concentration ($Bq\ m^{-3}$).

The source term, $S = \lambda_{Rn} C_{src}$, is related to the radon concentration in the material if there was no transport across the air-soil interface and the generation and removal within the soil had reached a balanced state. This term is usually defined as the concentration in the material at a large depth (Porstendörfer, 1994; López-Coto *et al.*, 2009):

$$C_{src} = \frac{\varepsilon \rho A_{Ra}}{\beta} \tag{3}$$

Where:

- ε Radon emanation.
- ρ Material density ($kg\ m^{-3}$).
- A_{Ra} Radium activity ($Bq\ kg^{-1}$).
- β Effective porosity.

Conversely, the radon removal term, $R = \lambda_{Rn} C_{Rn}$, can only be related to radon decay within the soil, which depends on the decay constant and the radon concentration at any given point in time or space.

Solution to equation (2) will be the combination of the solution for the homogenous equation plus a particular solution. First, we will find the homogeneous solution of the equation:

$$\frac{\partial^2 C_{Rn}}{\partial z^2} - \frac{\lambda_{Rn}}{D_B} C_{Rn} = 0 \tag{4}$$

The characteristic polynomial of this equation and its roots will be:

$$r^2 - \frac{\lambda_{Rn}}{D_B} \lambda_{Rn} = 0 \tag{5}$$

$$r = \pm \sqrt{\frac{\lambda_{Rn}}{D_B}} \tag{6}$$

Thus, solution to equation (4) will have the form:

$$C_{Rn}(z) = c_1 e^{rz} + c_2 e^{-rz} = c_1 e^{\sqrt{\frac{\lambda_{Rn}}{D_B}} z} + c_2 e^{-\sqrt{\frac{\lambda_{Rn}}{D_B}} z} \tag{7}$$

Where we can define the diffusion length as:

$$l_0 = \frac{1}{r} = \sqrt{\frac{D_B}{\lambda_{Rn}}} \tag{8}$$

Once we have solved the homogeneous part, we must find a particular solution. Making the second derivate equal to zero in eq. (2) yields:

$$C_{Rn}(z) = C_{src} \tag{9}$$

Finally, solution to equation (2) will be:

$$C_{Rn}(z) = C_{src} + c_1 e^{z/l_0} + c_2 e^{-z/l_0} \tag{10}$$

To obtain the expressions for c_1 andc_2, we must apply the boundary conditions $C_{Rn}(0) = C_{amb}$ and $C_{Rn}(L) = C_{src}$. Thus:

$$C_{Rn}(0) = C_{amb} = C_{src} + c_1 e^0 + c_2 e^{-0} = C_{src} + c_1 + c_2$$

$$c_1 = C_{amb} - C_{src} - c_2 \tag{11}$$

Applying (11) to the second boundary condition:

$$C_{Rn}(L) = C_{src} = C_{src} + c_1 e^{L/l_0} + c_2 e^{-L/l_0}$$

$$0 = (C_{amb} - C_{src} - c_2) e^{L/l_0} + c_2 e^{-L/l_0}$$

$$0 = (C_{amb} - C_{src})\, e^{L/l_0} - c_2 \left(e^{L/l_0} - e^{-L/l_0}\right)$$

$$c_2 = \frac{(C_{amb} - C_{src})\, e^{L/l_0}}{2senh(L/l_0)} \tag{12}$$

Now we can rewrite (11) as:

$$c_1 = C_{amb} - C_{src} - \frac{(C_{amb} - C_{src})\, e^{L/l_0}}{2senh(L/l_0)}$$

$$c_1 = \frac{(C_{amb} - C_{src})\, 2senh(L/l_0) - (C_{amb} - C_{src})\, e^{L/l_0}}{2senh(L/l_0)}$$

$$c_1 = \frac{(C_{amb} - C_{src}) \left(e^{L/l_0} - e^{-L/l_0}\right) - (C_{amb} - C_{src})\, e^{L/l_0}}{2senh(L/l_0)}$$

$$c_1 = \frac{(C_{amb} - C_{src}) e^{L/l_0} - (C_{amb} - C_{src}) e^{-L/l_0} - (C_{amb} - C_{src})\, e^{L/l_0}}{2senh(L/l_0)}$$

$$c_1 = -\frac{(C_{amb} - C_{src}) e^{-L/l_0}}{2senh(L/l_0)} \tag{13}$$

Summing it up, the behavior of radon concentration within the material in steady-state conditions will be determined by the following relations:

$$\boldsymbol{C_{Rn}(z) = C_{src} + c_1 e^{z/l_0} + c_2 e^{-z/l_0}} \tag{14}$$

$$\boldsymbol{l_0 = \sqrt{\frac{D_B}{\lambda_{Rn}}}} \tag{15}$$

$$\boldsymbol{c_1 = -\frac{(C_{amb} - C_{src}) e^{-L/l_0}}{2senh(L/l_0)}} \tag{16}$$

$$\boldsymbol{c_2 = \frac{(C_{amb} - C_{src})\, e^{L/l_0}}{2senh(L/l_0)}} \tag{17}$$

Where l_0 is the so called radon diffusion length. As an example, Figure 11 shows radon concentrations within the soil if we consider a gypsum soil with a radium activity $A_{Ra} = 50\ Bq\ kg^{-1}$, density $\rho = 1100\ kg\ m^{-3}$, emanation factor $\varepsilon = 0.1$ and effective porosity $\beta = 0.4$, under an radon free atmosphere, $C_{amb} = 0\ Bq\ m^{-3}$. Higher emanations, thus a higher radon source term C_{src}, will increase the maximum concentration inside the material, as more radon will be able to escape the grains and reach the pore space. On the other hand, the diffusion length affects how far can radon

travel within the soil. Higher diffusion lengths will cause a higher gradient, enhancing the radon transport and significantly decreasing the concentration at the interface air-soil.

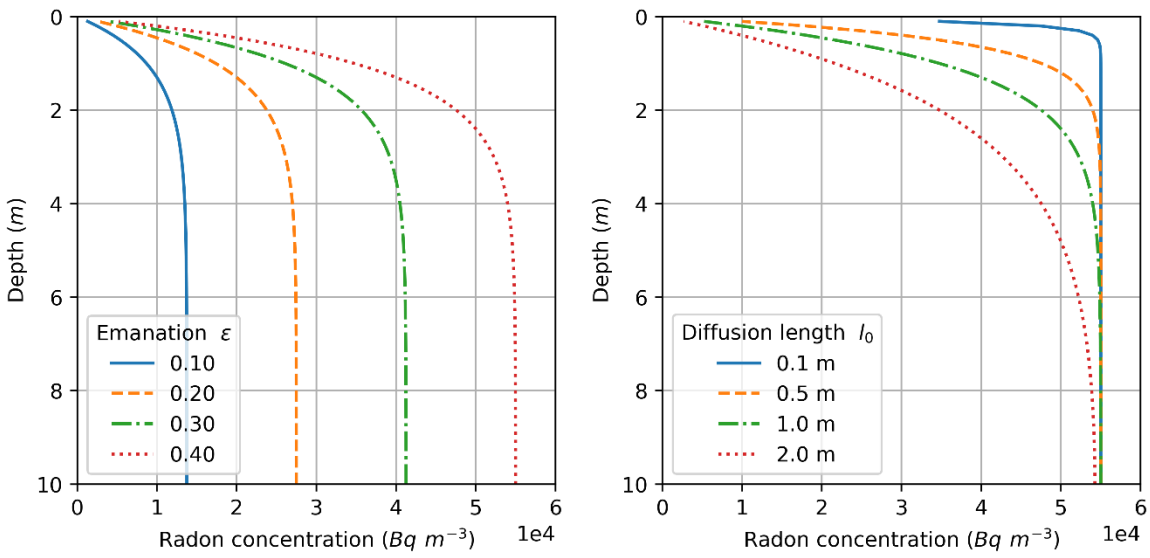

Figure 11. Radon concentration within the soil for the case of gypsum changing the emanation factor (left) and the diffusion length (right). While changing diffusion length, emanation is considered to be higher than normal, $\varepsilon = 0.4$, for better representation.

Deduction of the exhalation rate

The exhalation rate is defined as the rate at which radon escapes the material through its surface to the external air. Using Fick's first law:

$$E = -D_B \frac{\partial C_{Rn}(z)}{\partial z}\bigg|_{z=0} = -\lambda_{Rn} l_0^2 \frac{\partial C_{Rn}(z)}{\partial z}\bigg|_{z=0} \tag{18}$$

Thus:

$$E = -\lambda_{Rn} l_0^2 \left[\frac{c_1}{l_0} e^{z/l_0} - \frac{c_2}{l_0} e^{-z/l_0}\right]_{z=0} = -\frac{\lambda_{Rn} l_0^2}{l_0}(c_1 e^0 - c_2 e^0) = -\lambda_{Rn} l_0 (c_1 - c_2)$$

$$c_1 - c_2 = -\frac{(C_{amb} - C_{src})e^{-L/l_0} + (C_{amb} - C_{src})\, e^{L/l_0}}{2senh(L/l_0)}$$

$$c_1 - c_2 = \frac{(C_{amb} - C_{src})(e^{-L/l_0} + e^{L/l_0})}{2senh(L/l_0)}$$

$$c_1 - c_2 = \frac{(C_{amb} - C_{src})2\cosh(L/l_0)}{2senh(L/l_0)}$$

$$c_1 - c_2 = \frac{(C_{amb} - C_{src})}{tgh(L/l_0)} \tag{19}$$

As a result:

$$E = -\lambda_{Rn} l_0 \frac{(C_{amb} - C_{src})}{tgh(L/l_0)}$$

$$E = \frac{\lambda_{Rn} l_0}{tgh(L/l_0)} (C_{src} - C_{amb}) \tag{20}$$

This last expression can be further separated in two part representing the free exhalation rate, E_0, and a second term that addresses the reduction in the exhalation rate as the radon concentration on the outside changes. This is expected as diffusion must be proportional to the concentration difference between two points.

As a consequence:

$$E = \frac{\lambda_{Rn} l_0}{tgh(L/l_0)} C_{src} - \frac{\lambda_{Rn} l_0}{tgh(L/l_0)} C_{amb}$$

$$\boldsymbol{E = E_0 - \omega C_{amb}} \tag{21}$$

Where:

$$\boldsymbol{E_0 = \frac{\lambda_{Rn} l_0 \varepsilon \rho A_{Ra}}{\beta tgh(L/l_0)}} \tag{22}$$

$$\boldsymbol{\omega = \frac{\lambda_{Rn} l_0}{tgh(L/l_0)}} \tag{23}$$

The term E_0 is the so-called "Free Exhalation" which represents the maximum exhalation capacity of the material if there was no radon on the outside air. On the other hand, ω, represents the rate at which the radon exhalations is reduced by the outside concentration, and is related to the material geometry, diffusion length and diffusion constant of the material. This is effect is commonly called "back-diffusion" or "bound exhalation".

The behavior of equation (21) can be seen in Figure 12. Ambient radon concentration will decrease linearly the radon exhalation, although high concentrations must be reached to have a significant effect. Emanation will increase the free exhalation by a constant factor, as more radon reach the pore space and is able to travel towards the surface. Finally, diffusion length plays a different role, as it modulates the influence that radon ambient concentration has on the exhalation rate.

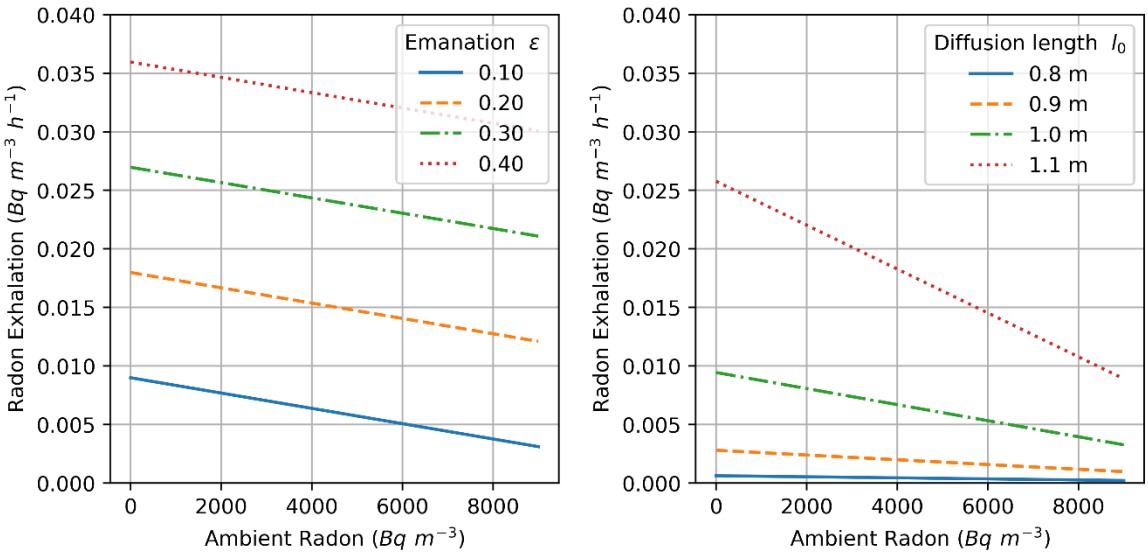

Figure 12. Radon exhalation for the case of gypsum changing the emanation factor (left) and the diffusion length (right), considering $\varepsilon = 0.1$.

2.2.2 Measurement Techniques

There are three basic approaches to measure radon exhalation: accumulation, flow through systems and adsorption. All three methods are based on the accumulation of radon inside a volume in direct contact with the surface to be measured. This volume is usually called accumulator or accumulation chamber. The three main methods to measure radon exhalation are described in the following sections.

Accumulation

As stated before, the accumulation method is based on the placement of a closed chamber over the surface to be measured, as depicted in Figure 13. Radon exhaled through the surface will be trapped inside the chamber and starts to accumulate inside it. Once enough time has passed, radon concentration will reach a steady state, approaching to a saturation concentration, which depends on the characteristics of the accumulation chamber and the exhalation of the material. Measuring the radon growth inside the chamber the accumulation curve can be registered. The exhalation rate can then be deduced fitting this curve to a known equation.

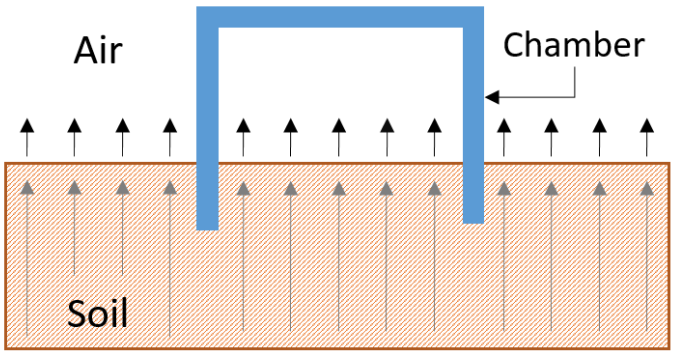

Figure 13. Scheme of the accumulation chamber method

Considering an homogenous concentration inside the chamber, the evolution of radon within an accumulation chamber is described by the following balance equation (Jonassen, 1983; López-Coto *et al.*, 2009; Seo *et al.*, 2018):

$$\frac{\partial C_{Rn}(t)}{\partial t} = \frac{S}{V}E(t) - \lambda_{Rn}C_{Rn}(t) - \lambda_l C_{Rn}(t) \tag{24}$$

Where:

- C_{Rn} Radon concentration (Bqm^{-3}).
- S Chamber-soil Surface (m^{-2}).
- V Accumulation Volume (m^{-3}).
- E Exhalation rate ($Bqm^{-2}s^{-1}$).
- λ_{Rn} Radon decay constant (s^{-1}).
- λ_l Radon leakage constant (s^{-1}).

This equation describes the balance between the radon sources, i.e. radon exhalation, and radon sinks, i.e. radon radioactive decay and leakages. It is important to reiterate that the exhalation rate will not be constant in time due to the radon increase inside the chamber and the subsequent decrease in the diffusion transport from the soil to the accumulation chamber.

Applying equation (21) to (24):

$$\frac{\partial C_{Rn}(t)}{\partial t} = \frac{S}{V}E_0 - \frac{S}{V}\omega C_{Rn}(t) - \lambda_{Rn}C_{Rn}(t) - \lambda_l C_{Rn}(t) \tag{25}$$

The second term on the right side describes the reduction in the exhalation as the radon concentrations increase inside the chamber. This effect appears as a virtual radon sink in the balance equation and is commonly referred to as bound-exhalation, where:

$$\frac{S}{V}\omega = \frac{S\lambda_{Rn}l_0}{Vtgh(L/l_0)} = \lambda_b \tag{26}$$

This effect depends on the geometry of the accumulation chamber, the radon diffusion length within the soil, and the depth of the soil.

As a consequence, the balance equation can be rewritten as:

$$\frac{dC_{Rn}(t)}{dt} = \frac{E_0\,S}{V} - (\lambda_{Rn} + \lambda_l + \lambda_b)C_{Rn}(t) \tag{27}$$

$$\frac{dC_{Rn}(t)}{dt} = \frac{E_0\,S}{V} - \lambda_{ef}C_{Rn}(t) \tag{28}$$

Where:

- $C_{Rn}(t)$ Concentración de radón ($Bq\ m^{-3}$).
- E_0 Free exhalation rate ($Bqm^{-2}h^{-1}$).
- λ_{ef} Effective time constant (s^{-1}).
- λ_{Rn} Radon decay constant (s^{-1}).
- λ_l Leakage constant (s^{-1}).
- λ_b Bound exhalation constant (s^{-1}).
- S Accumulation chamber exhalation surface (m^{-2}).
- V Accumulation chamber effective accumulation volume (m^{-3}).

In this case, the free exhalation rate, E_0, represents the radon exhalation if no accumulator was placed. Rearranging terms:

$$\frac{dC_{Rn}(t)}{\frac{E_0\,S}{V} - \lambda_{ef} C(t)} = dt \tag{29}$$

Integrating:

$$\frac{\ln\left(\frac{E_0\,S}{V} - \lambda_{ef} C_{Rn}(t)\right)}{-\lambda_{ef}} = t + c_0$$

where c_0 is the integration constant. Working on the equation:

$$\ln\left(\frac{E_0\,S}{V} - \lambda_{ef} C_{Rn}(t)\right) = -\lambda_{ef} t - \lambda_{ef} c_0$$

$$\frac{E_0\,S}{V} - \lambda_{ef} C_{Rn}(t) = e^{-\lambda_{ef} c_0} e^{-\lambda_{ef} t} = c_1 e^{-\lambda_{ef} t}$$

$$C_{Rn}(t) = \frac{E_0 S}{\lambda_{ef} V} - \frac{c_1}{\lambda_{ef}} e^{-\lambda_{ef} t} \tag{30}$$

To find the integration constant c_1 initial conditions must be used. It is reasonable to suppose that at the beginning of the accumulation there is an arbitrary radon concentration inside the chamber, C_0. Thus:

$$C_{Rn}(0) = C_0 = \frac{E_0 S}{\lambda_{ef} V} - \frac{c_1}{\lambda_{ef}} e^0 = \frac{E_0 S}{\lambda_{ef} V} - \frac{c_1}{\lambda_{ef}}$$

$$\frac{c_1}{\lambda_{ef}} = \frac{E_0 S}{\lambda_{ef} V} - C_0 \tag{31}$$

Then, combining this with (30):

$$C_{Rn}(t) = \frac{E_0 S}{\lambda_{ef} V} - \left(\frac{E_0 S}{\lambda_{ef} V} - C_0\right) e^{-\lambda_{ef} t} = \frac{E_0 S}{\lambda_{ef} V} + \left(C_0 - \frac{E_0 S}{\lambda_{ef} V}\right) e^{-\lambda_{ef} t}$$

$$\boldsymbol{C_{Rn}(t) = C_{sat} + (C_0 - C_{sat}) e^{-\lambda_{ef} t}} \tag{32}$$

$$\boldsymbol{C_{sat} = \frac{E_0 S}{\lambda_{ef} V}} \tag{33}$$

Where C_{sat} is the saturation concentrations of the system, reached when $t \to \infty$.

In most cases, the initial concentration can be neglected when compared to the saturation concentration. In these cases, the approximation $C_0 \ll C_{sat}$ can be used and (32) rewritten as:

$$\boldsymbol{C(t)|_{C_0 \ll C_{sat}} = C_{sat}(1 - e^{-\lambda_{ef} t})} \tag{34}$$

This is an expression typically used in the literature (Jonassen, 1983; Aldenkamp *et al.*, 1992; Onishchenko, Zhukovsky and Bastrikov, 2015; Seo *et al.*, 2018). As seen in eq. (33), a higher saturation concentration parameter implies that there is a higher exhalation rate or a bigger air-soil interface area, increasing the amount of radon that can enter the accumulator. The volume or the effective decay constant have an effect on the effective capacity of the accumulator to store radon, so the saturation concentration will be inversely proportional to them.

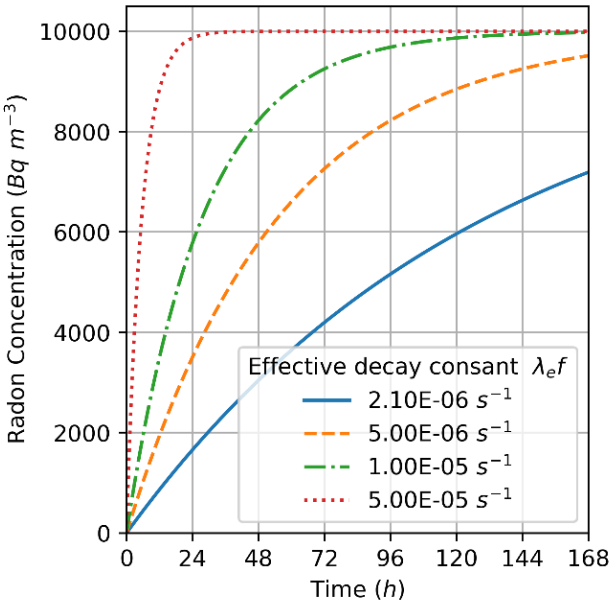

Figure 14. Radon concentration in an initially radon free accumulation chamber ($C_0 = 0\ Bq\ m^{-3}$) varying the effective decay constant with $C_{sat} = 10\ 000\ Bq\ m^{-3}$.

The λ_{ef} parameter is critical as it defines how much time the system will need to reach the steady state. Accumulation systems with lower λ_{ef} will grow linearly in the first moments of the accumulation (Figure 14). In these cases, the exponential term of equation (34) can be approximated by $1 - \lambda_{ef}t$, obtaining the expression for the linear approximation:

$$\boldsymbol{C(t)|_{C_0 \ll C_{sat}\ and\ \lambda_{ef}t \ll 1} \approx C_{sat}\lambda_{ef}t} \tag{35}$$

In all cases, the free exhalation rate, E_0, can be obtained using its relationship with the saturation concentration and the effective decay constant:

$$\boldsymbol{E_0 = C_{sat}\lambda_{ef}\frac{V}{S}} \tag{36}$$

After fitting the radon growth to one of the exponential fits (eq. (32) or (34)) or the linear fit (eq. (35)), the free exhalation rate can be obtained using (36).

Flow through

The flow through method is similar to the accumulation but it forces a continuous air removal to reach the steady state faster than in the classical accumulation technique. The air removal rate must be chosen carefully since, if it is too high, radon concentrations could be extremely low, increasing the uncertainties due to low counting rates. On the other hand, higher removal rates could cause a pressure difference between the interior and exterior of the chamber, producing a pumping effect and artificially increasing the exhalation rate (Hosoda *et al.*, 2011).

Equation (28) needs to be modified to include the introduction of ambient air and the removal of air inside the chamber:

$$\frac{dC_{Rn}(t)}{dt} = \frac{E_0\ S}{V} + \frac{\nu}{V}C_{Amb}(t) - \lambda_{ef}C_{Rn}(t) - \frac{\nu}{V}C_{Rn}(t) \tag{37}$$

Where ν is the flow rate at which the air inside the chamber is renewed.Considering that the radon increase due to the introduction of exterior air is negligible, we can rearrange terms, obtaining:

$$\frac{dC_{Rn}(t)}{dt} = \frac{E_0\, S}{V} - \left(\lambda_{ef} + \frac{\nu}{V}\right) C_{Rn}(t) \tag{38}$$

The solution to equation (37) is analogous to (28):

$$C_{Rn}(t) = C_{sat} + (C_0 - C_{sat})e^{-\left(\lambda_{ef}+\frac{\nu}{V}\right)t} \tag{39}$$

$$C_{sat} = \frac{E_0\, S}{V\left(\lambda_{ef} + \frac{\nu}{V}\right)} \tag{40}$$

Ideally, the quotient between the flow rate and the chamber volume, $\frac{\nu}{V}$, will be chosen so that the approximation $\lambda_{ef} \ll \frac{\nu}{V}$can be applied. This will allow to neglect the effect of chamber leaks, bound-exhalation and radon decay, making the usage of the flow-through system more operative.

In addition, if the initial radon concentration is also negligible, $C_0 \ll C_{sat}$, equation (39) and (40) come to be:

$$C(t)|_{\lambda_{ef}\ll\frac{\nu}{V}\ and\ C_0\ll C_{sat}} \approx C_{sat}\left(1 - e^{-\frac{\nu}{V}t}\right) \tag{41}$$

$$C_{sat} \approx \frac{E_0\, S}{\nu} \tag{42}$$

And the free exhalation can be obtained using the saturation concentration and the flow rate as:

$$E_0 \approx \frac{\nu}{S} C_{Sat} \tag{43}$$

Adsorption

This method takes advantage of a medium with adsorption capacity, such as activated charcoal, to trap radon within its pores. The adsorbent material is placed inside a canister which is then placed over the surface to investigate. In the case of activated charcoal, the material has to be purged prior to deployment to remove radon, moisture and other contaminants that may be present. After purging, the canister is sealed to ensure it remains cleaned until its use.

The exposure time to the source may vary between 3 hours to several days, depending on the measurement objective and the soil characteristics. After its exposure, the canisters have to be sealed again, following for a period of three hours to allow radon progeny to reach equilibrium with radon. Afterwards, ^{214}Pb and ^{214}Bi activity can be measured by gamma spectroscopy.

Radon exhalation can be obtained using the expression (Spehr and Johnston, 1983; IAEA, 2013):

$$E = \frac{N\, t_c \lambda_{Rn} e^{\lambda_{Rn} t_d}}{\varepsilon\, S\, (1 - e^{-\lambda_{Rn} t_e})\, (1 - e^{-\lambda_{Rn} t_c})} \tag{44}$$

Where:

- N Net count rate, after background subtraction (Bq)
- λ_{Rn} Radon decay constant (s^{-1}).
- ε Counting efficiency of the system.

- S Surface of the canister (m^2).
- t_c Counting period (s).
- t_d Delay period from end of exposure to beginning of counting (s).
- t_e Period of exposure to the radon source (s).

2.3 Reference exhalation boxes

In order to test the radon exhalation methods, a material with a known or controlled exhalation had to be used. To achieve this, a reference exhalation box was designed and built using phosphogypsum (PG) from the repository located near Huelva. The exhalation boxes were made out of a polypropylene rectangular container, with 0.44 m^2 and 174 L of capacity (77x57x39.7 cm), dimensions big enough to fit small accumulation chamber inside (Figure 15a). Polypropylene was chosen as the material for the boxes due to its lower permeability to radon. A cover was designed to air-tightly close the container and use the interior as an accumulation chamber itself (Figure 15b). This way, the exhalation rate of the PG layer as a whole could be measured without disturbing it by placing accumulation chamber.

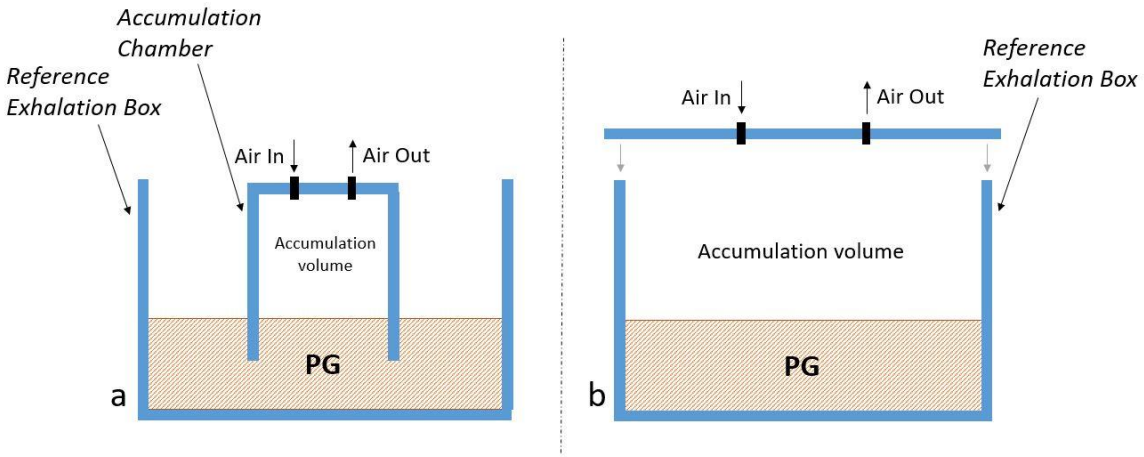

Figure 15. Scheme of an insertion chamber placed inside an open reference exhalation chamber (a), and a scheme of a closed reference exhalation chamber.

The PG was retrieved from the repository and stored in seven bags with about 25 kg of material each. These bags were homogenized independently, and its radium concentration was measured. Afterwards, 900 g of PG from each bag were placed inside the polypropylene box iteratively, homogenizing its contents at every step, until the desired amount of PG was reached.

The exact procedure followed the next steps:

1. 900 g were taken from each bag and placed in the reference exhalation box.
2. The PG was thoroughly homogenized, combining the already placed PG with the newly added material.
3. Repeat until the desired PG quantity is reached.

Following this method, two reference exhalation boxes, RB1 and RB2 from now on, were built. RB1 contains 35 kg of phosphogypsum in a 6 cm height layer. RB2 contains 70 kg in a 13 cm cover. The volumes left for radon accumulation were 148.1 L for RB1 and 117.2 L for RB2. For each of these reference boxes, 4 samples were taken at four different points and from the middle of the PG layer. These samples were measured by gamma spectroscopy to ensure that the radium content, and

thus the radon exhalation rate, was homogenous across the PG layer. The measured radium on each reference box was $451 \pm 7\ Bq\ kg^{-1}$ and $420 \pm 8\ Bq\ kg^{-1}$, for RB1 and RB2, respectively.

Due to the humidity content of the PG, the exhalation of the reference boxes was expected to change over time, as the material will dry and reduce its humidity. The exhalation rate was monitored by routinely performing measurements with the reference box and accumulation chambers until a steady-state was reached, which took 1 month for RB1 and 3 months for RB2, approximately. In addition, routine measurements were made after the exhalation values stabilized, to ensure its constancy over time.

After almost 100 experiments on the reference exhalation boxes, the reference exhalation rate was obtained by fitting the radon growth of each experiment to equation (32) and computing the average of all experiments performed. The exhalation rate was measured with different devices, two Alphaguards, one Rad 7 and one Radon Scout. A student's t-test was employed and no differences across devices were found. Combining all of these experiments, the reference exhalation rate on RB1 was found to be $E_0|_{RB1} = 47.7 \pm 0.7\ Bq\ m^{-2}\ h^{-1}$(48 experiments), while on RB2 it was $E_0|_{RB2} = 84.5 \pm 0.9\ Bq\ m^{-2}\ h^{-1}$ (44 experiments).

To verify these results, the theoretical exhalation rate was calculated using the expression (López-Coto *et al.*, 2009):

$$E_0 = \varepsilon \rho \lambda_{Rn} C_{Ra} z_0 \tag{45}$$

Where:

- ε Emanation factor.
- ρ Density ($kg\ m^{-3}$).
- λ_{Rn} Radon decay constant (s^{-1}).
- C_{Ra} Radium concentration in the soil ($Bq\ kg^{-3}$).
- z_0 Height of the emitting layer (m).

This equation is only valid when the height of the material is small when compared to the radon diffusion length. In materials like PG the diffusion length is considered to be 1 m, although this value depends on the humidity content (Rogers and Nielson, 1991; Keller, Hoffmann and Feigenspan, 2001). To compute the rest of the values needed, different methods were used. First, once the reference boxes were finished, four PG samples were taken from each box from different points of the emitting surface. This samples were used to measure the radium content by gamma spectroscopy. On the other hand, layer height was measured directly on the box and combined with the surface to obtain the density. Finally, the emanation factor was extracted from López-Coto et al., 2014.These results can be seen in Table 1.

Table 1. Values needed to obtain the theoretical exhalation rate.

Reference Box	ε	ρ ($kg\ m^{-3}$).	C_{Ra} ($Bq\ kg^{-3}$)	z_0 (cm)	Theoretical E_0 ($Bqm^{-2}h^{-1}$)
RB1	0.20 ± 0.04	1080 ± 10	451 ± 7	5.95 ± 0.05	44 ± 9
RB2	0.20 ± 0.04	1011 ± 3	420 ± 8	13.00 ± 0.03	82 ± 17

Theoretical and experimental result are quite similar, pointing out that the design experiment was appropriate and provided an accurate way of stablishing a reference exhalation rate where further experimentation can be carried out.

2.4 Measurement stations and ARMON Support System

Two atmospheric radon measurement stations were built and managed, one located inside the urban area of Huelva, El Carmen station, and a second one to the south of the PG repository, La Rabida station (Figure 16). Among many other devices to monitor environmental radioactivity, the stations host an ARMON atmospheric radon measurement device, which was briefly described in a previous chapter.

Data from the observatory of AEMET (*Agencia Española de Meteorología*: Spanish Agency for Meteorology) located near the city area was employed to characterize the meteorological variables in the area of study. This station measures local atmospheric variables such as temperature, humidity, pressure and wind speed and direction, among others.

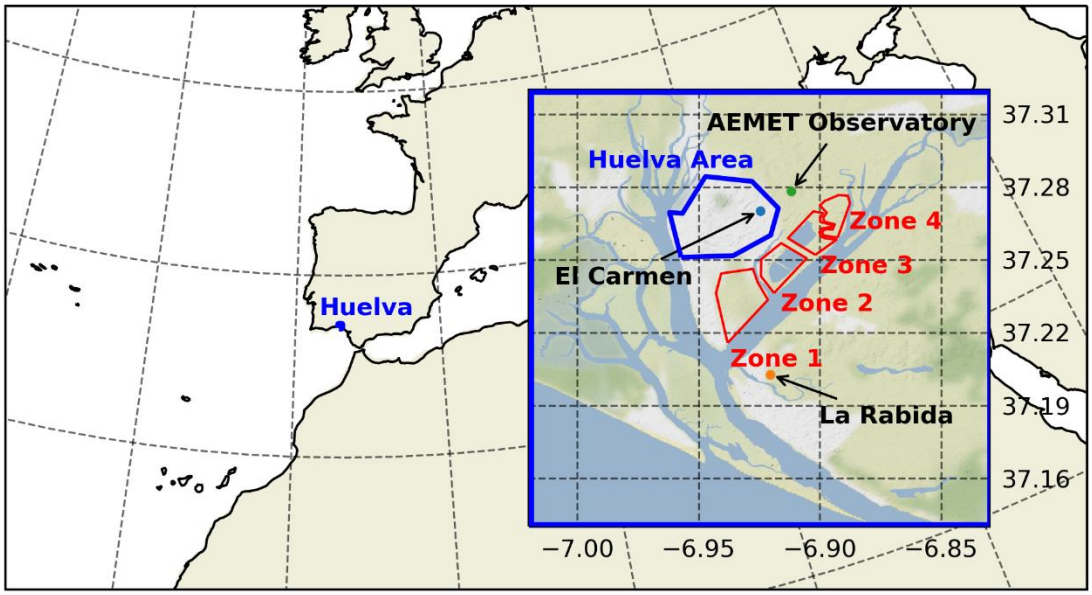

Figure 16. Location of the measurement stations in the area of study.

The complete scheme of the El Carmen ARMON Support System is shown in Figure 17. Firstly, sampled air is pumped inside the system, going through a purging setup to remove water, oil and particles. The flow rate is controlled by an electro-valve. At the same time, a compressor is used to introduce a similar secondary airflow at 6 bars, which is then guided to an air pre-dryer followed by a particle filter. Afterwards, the sampled air and the secondary airflow are guided into a nafion tube, which transfers the humidity of the former to the latter. After this process, the sampled air has an optimal humidity content and enters the ARMON measurement chamber. A particle filter is located at the entrance of the ARMON to ensure that no undesired radon progeny alters the measurement.

La Rabida ARMON Support System is almost equivalent to El Carmen's (Figure 18). In this case, the nafion tube is substituted by a series of silica gel tubes. The air circulates through only two of the silica gel tubes at a time, switching between tubes every eight hours, ensuring a correct drying of the air and an adequate flow.

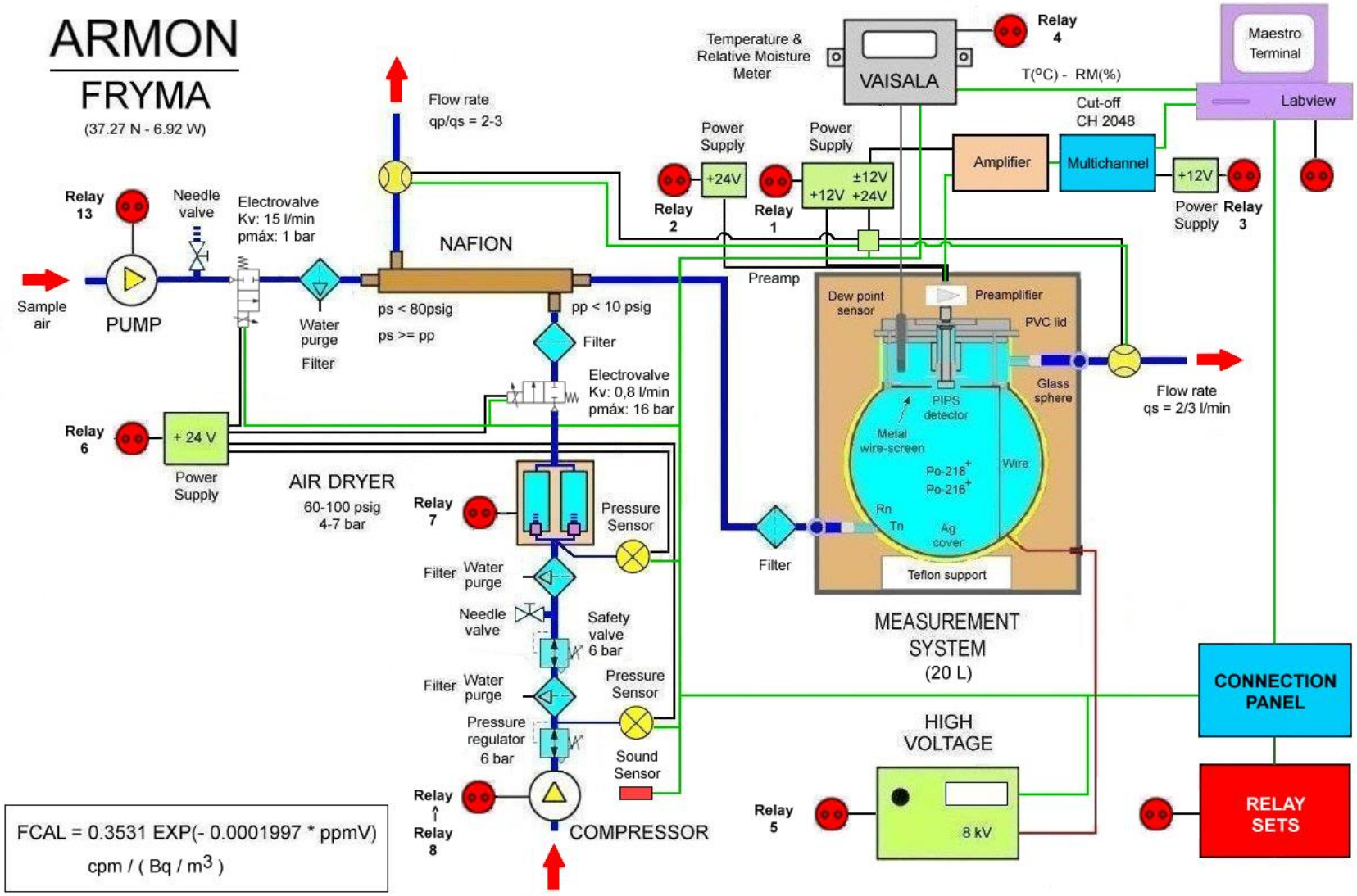

Figure 17. Scheme of the ARMON support system on El Carmen station

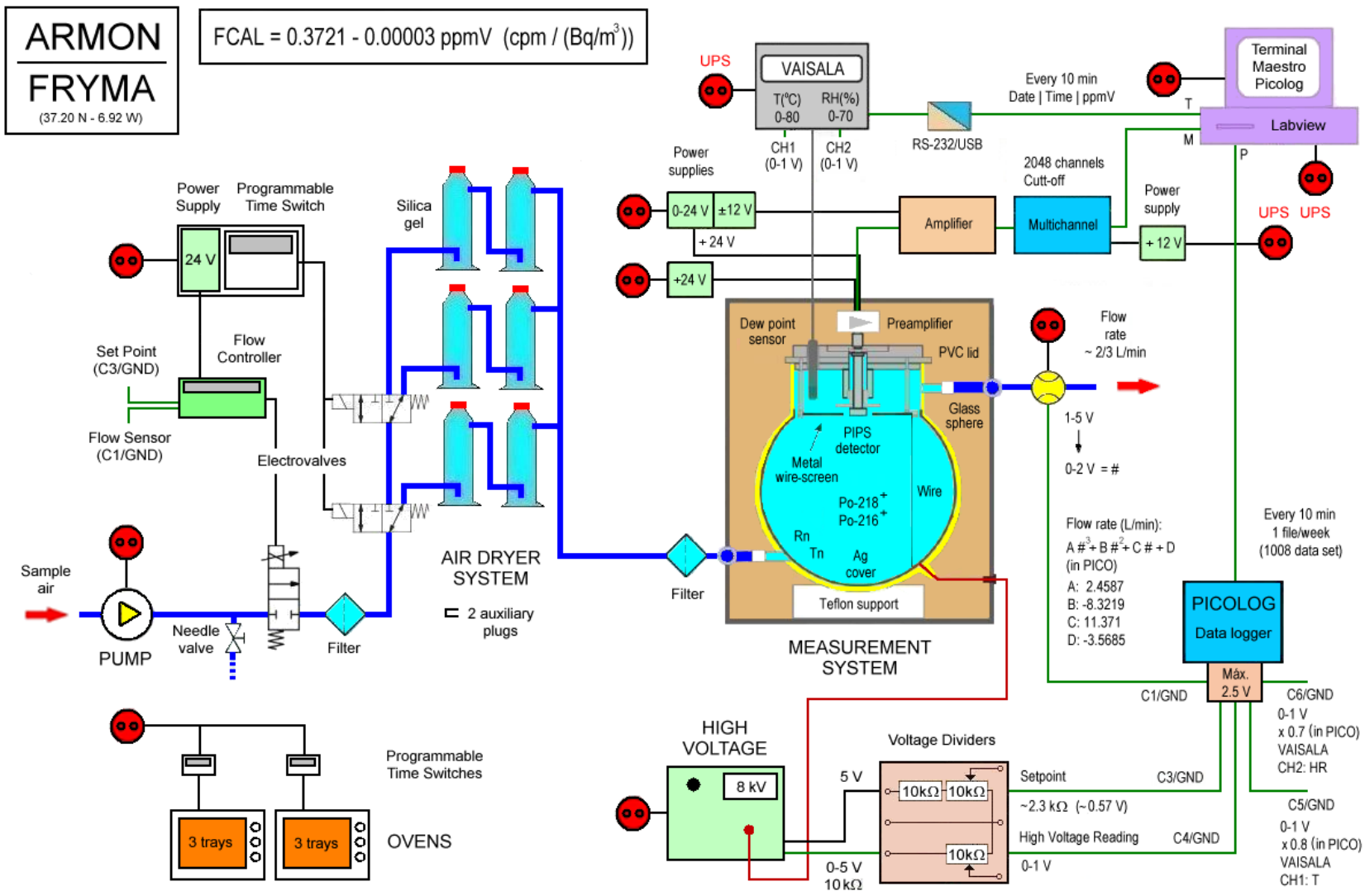

Figure 18. Scheme of the ARMON support system on La Rabida station.

The LABVIEW program was employed to develop an application including a virtual console and a quantification routine of hourly radon concentrations. The application has a virtual console that can be accessed remotely, providing information about the general state on the system and radon concentrations. In the case of El Carmen, the remote access allows to control the system parameters, like the intake flowrate. VAISALA devices were used to monitor ambient parameters like temperature and humidity.

Once radon reaches the ARMON detection volume, it starts to decay and its concentration can be calculated. Firstly, the measured signal goes through a preamplifier, that amplifies the signal looking for a better signal-noise ratio in the electronic chain. Secondly, an amplifier, gives each signal a Gaussian shape. Finally, signals reach a multichannel analyzer that generates a square signal for each one. The resulting signals are classified by their width, which is related to the energy of the alpha particle, thus providing an alpha spectrum. This information is passed to the MAESTRO software, which stores and represents the spectrum to be easily accessible in the future. A qualitative example of a typical alpha spectrum in log scale is shown in Figure 19.

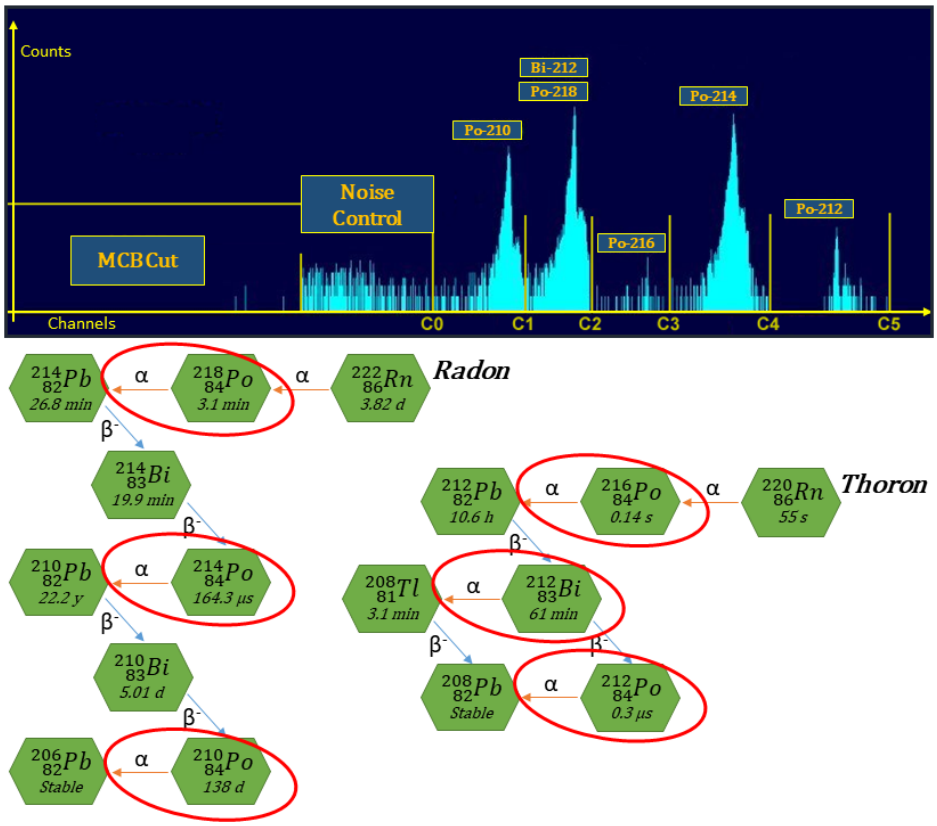

Figure 19. Example of a typical alpha spectrum in log scale registered by MAESTRO and the decay chain of radon and thoron.

As stated previously, the radon concentration can be deduced by the count rate of its daughter ^{218}Po (6.0 MeV). However, as seen in Figure 19, this signal is really close from the counts due to ^{212}Bi alpha decay (6.1 MeV), so they must be deconvoluted first. ^{212}Bi belongs to the thoron decay chain and mostly disintegrates by either alpha-decay, producing ^{208}Tl (35.94 %), or beta-decay, producing ^{212}Po (55.37 %). As a consequence, the ^{212}Bi counts can be deduced from its daughter, multiplying ^{212}Po counts by the proportion between the ^{212}Bi → ^{208}Tl emission probability (35.94 %) over the ^{212}Bi → ^{212}Po emission probability (64.06 %), which results in a factor of 0.561.

Additionally, since the system efficiency depends on humidity, a parametrization inside the calibration factor must be included to account for humidity variations between 0 and 2000 ppmV (Vargas, Ortega and Matarranz, 2004). All factors considered, the equations that provides ^{222}Rn concentration is:

$$C_{Rn} = (N_{Po218+Bi212} - 0.561 \cdot N_{Po212}) \frac{60}{F\,\tau} \quad (46)$$

Where:

- C_{Rn} Radon concentrations ($Bq\ m^{-3}$)
- $N_{Po218+Bi212}$ Counts due to ^{218}Po and ^{212}Bi (Bq).
- N_{Po212} Counts due to ^{212}Po (Bq).
- F Calibration factor (cpm/(Bq m^{-3})).
- τ Live counting time (s)

2.5 Software, datasets, models and code

Overall, approximately 400 radon exhalation experiments were carried out, and several years of atmospheric radon and other atmospheric variables were analyzed during this thesis. Several software tools were employed such as Python programming language or Microsoft excel, in addition to simulations models like WRF (Weather Research and Forecasting), FLEXPART (FLEXible TRAjectory model) and FLEXPART-WRF, or HYSPLIT (Hybrid Single Particle Lagrangian Integrated Trajectory model). Datasets from global reanalysis models such as ERA5, supported by the European Centre for Medium-Range Weather Forecast (ECMWF) were used as well.

2.5.1 Reanalysis models and WRF model

In order to analyze the behavior of atmospheric radon, it was often needed to study the atmospheric conditions. The atmospheric dynamic in the city of Huelva is governed by synoptic and mesoscale mechanisms. For analyzing the larger synoptic scale, a global reanalysis model is best suited. ERA5 is a climate reanalysis dataset that provides hourly estimates on a 30 km horizontal grid for a large number of atmospheric, land and oceanic climate variables. The model includes 137 sigma levels from the surface up to a height of approximately 80 km. ERA5 combines large amounts of observations into global estimates using advanced modelling and data assimilation systems (Hersbach *et al.*, 2020).

When ERA5 model resolution was not enough, WRF model were used to provide atmospheric information on a finer grid, both temporarily or spatially, based on the information provided by ERA5 or other global reanalysis models. WRF model is a next-generation mesoscale weather prediction system that features two dynamical cores, a data assimilation system and a software architecture that supports parallel computation. The model has been developed by a partnership of the National Center for Atmospheric Research (NCAR), the National Oceanic and Atmospheric Administration (represented by the National Centers for Environmental Prediction (NCEP) and the Earth System Research Laboratory), the U.S. Air Force, the Naval Research Laboratory, the University of Oklahoma, and the Federal Aviation Administration (FAA) (Skamarock *et al.*, 2008).

WRF allows the user to define the output grid resolution for the simulation and provides a myriad of parametrizations to simulate the atmosphere with different approximations of atmospheric dynamics systems. To ensure that the provided information was accurate, sensibility analysis was

carried out using AEMET stations measurements. This allowed to choose the best set of parameters to reproduce the atmospheric conditions in the area of study.

2.5.2 FLEXPART and HYSPLIT

The study of the origin of air masses is often a useful tool to analyze the behavior of any atmospheric pollutant, as it can uncover its sources or pathways into the area of study. Air masses trajectories were analyzed to study radon transport into Huelva, allowing to analyze which pathways are associated with higher radon concentrations or to relevant atmospheric situations. To do this, two trajectory models were used: FLEXPART and HYSPLIT.

FLEXPART (FLEXible PARTicle dispersion model) is a Lagrangian transport and dispersion model for multi-scale atmospheric transport modelling and analysis. This model simulates the transport, diffusion and deposition of atmospheric tracers released from a defined source. It also accounts for radioactive decay or first-order chemical reactions of the tracers. This model can be run forwards or backwards or time, allowing to optimize the simulation depending on the number of receptor or sources (Pisso *et al.*, 2019).

On the other hand, HYSPLIT (Hybrid Single-Particle Lagrangian Integrated Trajectory) model is a complete system for computing simple air parcel trajectories, as well as complex transport, dispersion, chemical transformation, and deposition simulations. The model computation algorithm is a hybrid between the Lagrangian and Eulerian approaches. This hybrid configuration allows the model run faster than other Lagrangian models, performing a higher number of simulations in the same span of time (Draxler *et al.*, 2018).

Both of these models require meteorological fields to accurately reproduce the state of the atmosphere during its simulations. In general, ERA5 datasets were employed, as the models are already prepared to work with ECMWF datasets. In some cases, when transport simulations with higher resolution were required, a variant of the FLEXPART model, FLEXPART-WRF, were used (Brioude *et al.*, 2013). This iteration of the lagrangian transport model is specially prepared to work with WRF output as its own input, effectively increasing its spatial and temporal resolutions as high as the WRF simulations can be.

2.5.3 Data treatment and python coding

The main software tool used to retrieve, organize and analyze all data used in this work was Python programming language. More than 4000 lines of operative code were written by the author throughout this work, using open source packages maintained by the community like pandas, xarray or matplotlib. An extensive reference list of all employed packages is provided in the references.

Radon exhalation measurements

Radon exhalation measurement had to be derived from the evolution of radon concentration during experiments that lasted several hours. These measurements could be made on different reference exhalation boxes, with several accumulators and using different radon measurement devices, where each of them used a different format to store its data. To handle all of this information, several specific python scripts had to be written to extract the exhalation measurement depending on the instrument employed, the reference box or the accumulator. To organize the radon concentration data of the 400 experiments, the files were read iteratively applying the exponential or linear fit analysis, saving the results to an excel file. Afterwards, statistical analysis code could be used to extract cleaned information understandable by the researcher.

It is important to note that data files were named following a specific format to indicate information about the experiment conditions. The general file naming convention was:

YYYY-MM-DD-HHMM_DEVICE_ACCUMULATOR_SOIL_METHOD_OTHERS.txt

This allowed the code to easily separate the information using the underscores ('_'). The first part refers to the starting time of the measurement, providing exactly 4 digits to the year, 2 digits for the month and day, and another 4 digits for the starting time. This first part also served as a unique identifier for each experiment, ensuring the traceability and identification of each measurement experiment. The following pieces referred to the device, accumulation chamber, soil and method used to measure the exhalation. More information could be added to the end in special cases. This method allows to store the information relative to each device and accumulator on a different file, and ensures that the correct parameters, such as volume or surface of the accumulator, was used for each file.

As an example, a file named '2019-12-21-1431_R7_V10_RB1_CC.txt'would contain the data of an experiment started at 14:31 on December 21st, 2019, using the closed chamber accumulation method (CC), performed on the reference exhalation box RB1, using the accumulation chamber V10 and the Rad 7 device.

When applying the desired fit method to the measurements, the code was designed to grant the researcher freedom to define the fit parameters. It allowed to choose what fit to use (exponential or linear), whether to consider initial concentration or not, the duration to use for the fitting or the number of initial points to exclude from the fit. This way, the code could compute within minutes the results of any request that the researcher might want to test over the 400 exhalation experiments. As an example, the researcher could apply the exponential fit with zero initial concentration, using only the first 2 hours of accumulation data but excluding the first 10 minutes of measurements, or any variation of those parameters.

Radon and meteorological experimental measurement

The FRyMA stations provided hourly radon measurements that had to be cleaned from outliers and resampled to fill-in any voids that may appear. This information was coupled together with meteorological data from a nearby AEMET observatory, such as temperature, pressure, relative humidity, wind speed and wind direction. Whenever needed, output information from other models was also extracted and normalized to the hourly radon measurement timestamps using code written in python programming language.

After the measurements were processed, visual representations and statistics were computed as well using python. Clustering techniques were also applied using tools written in this language. The use of this programming language allowed to apply the same analysis over different subsets of the data easily, modifying the analysis and plots to a high degree of freedom.

Models and reanalysis datasets

Simulations by either WRF, FLEXPART, FLEXPART-WRF or HYSPLIT required large amounts of global datasets to be successfully ran. The download and management of such datasets were handled using python. The CDS (Copernicus Climate Data Storage system) provides example python scripts to automatically download ERA5 datasets with personalized parameters such as area of interest, date or the specific variables to be downloaded.

Input and output from these models were often in NETCDF format. This file type helps in compressing large amounts of information into manageable files. As an example, a WRF week

simulation of the area of study could produce between 100 to 500 Gb of information, depending on the specific spatial and time resolutions employed in the simulation. To extract comprehensive information from these runs, several scripts were made to easily plot maps and time series of the simulations.

A special mention has to be made for the specific case of FLEXPART and FLEXPART-WRF. Due to the complex operation of this model, a special suit of software tools was developed to easily prepare, run and understand it's the output of its simulations. An object-oriented programming approach was chosen to develop these tools, defining an object class that offered the versatility to approach different kinds of simulations and outputs. More than 2000 lines of code were dedicated to this endeavor, providing the functionality to iteratively prepare and run simulations with slight modification in its parametrizations, merge different simulations into one or produce back-trajectories and time series plots in, apparently to the user, just one line of code.

TRABAJOS CIENTÍFICOS

Los trabajos científicos que forman parte de los capítulos 3, 4, 5 y 6 han sido retirados de la tesis debido a restricciones relativas a derechos de autor. Dichos artículos han sido sustituidos por su referencia bibliográfica, enlace al artículo y resumen.

- Gutiérrez-Álvarez, J.E. Martín, J.A. Adame, C. Grossi, A. Vargas, J.P. Bolívar, Applicability of the closed-circuit accumulation chamber technique to measure radon surface exhalation rate under laboratory conditions, Radiation Measurements, Volume 133, 2020, 106284, https://doi.org/10.1016/j.radmeas.2020.106284.

Enlace al artículo: https://doi.org/10.1016/j.radmeas.2020.106284

RESUMEN:
A layer of phosphogypsum was placed at the bottom of two large volume boxes. This system allowed to measure the surface radon exhalation from phosphogypsum without altering the emitting material. The limits and optimal setup of the closed-circuit accumulation chamber technique were thoroughly studied. More precisely, the performance of different radon exhalation fitting methods was analyzed in the reference exhalation boxes, employing different measurement devices and three smaller operational accumulation chambers. As expected, the best approach to obtain the radon exhalation rate depends upon the effective decay constant of the measurement system and the time employed to perform the measurement. The time until the linear approximation can no longer be applied was scrutinized. Although this approximation is usually applied routinely in the literature, the effective time constant of the chamber is often not low enough for the linear fit to be applied safely, providing statistically acceptable measurements that can lead to significative underestimations of the radon exhalation rate.

- Gutiérrez-Álvarez, J.L. Guerrero, J.E. Martín, J.A. Adame, J.P. Bolívar, Influence of the accumulation chamber insertion depth to measure surface radon exhalation rates, Journal of Hazardous Materials, Volume 393, 2020, 122344, https://doi.org/10.1016/j.jhazmat.2020.122344.

Enlace al artículo: https://doi.org/10.1016/j.jhazmat.2020.122344

RESUMEN:
A common method to measure radon exhalation rates relies on the accumulation chamber technique. Usually, this approach only considers one-dimensional gas transport within the soil that neglects lateral diffusion. However, this lateral transport could reduce the reliability of the method. In this work, several cylindrical-shaped accumulation chambers were built with different heights to test if the insertion depth of the chamber into the soil improves the reliability of the method and, in that case, if it could limit the radon lateral diffusion effects. To check this hypothesis in laboratory, two

reference exhalation boxes were manufactured using phosphogypsum from a repository located nearby the city of Huelva, in the southwest of Spain. Laboratory experiments showed that insertion depth had a deep impact in reducing the effective decay constant of the system, extending the interval where the linear fitting can be applied, and consistently obtaining reliable exhalation measurements once a minimum insertion depth is employed. Field experiments carried out in the phosphogypsum repository showed that increasing the insertion depth could reduce the influence of external effects, increasing the repeatability of the method. These experiments provided a method to obtain consistent radon exhalation measurements over the phosphogypsum repository.

- Gutiérrez-Álvarez, J.L. Guerrero, J.E. Martín, J.A. Adame, A. Vargas, J.P. Bolívar, Radon behavior investigation based on cluster analysis and atmospheric modelling, Atmospheric Environment, Volume 201, 2019, Pages 50-61, https://doi.org/10.1016/j.atmosenv.2018.12.010.

Enlace al artículo: https://doi.org/10.1016/j.atmosenv.2018.12.010

RESUMEN:

Radon measurements were performed in Huelva, a city located near a phosphogypsum repository in the SW of the Iberian Peninsula, between March 2015 and March 2016. The mean values of this gas oscillate between 5.6 and 10.9 Bq m−3 and maximum ranges between 36.4 and 53.4 Bq m−3. Radon shows the expected monthly variation with higher levels in November and December. Typical daily evolutions were also observed, with maximum between 06:00 and 08:00 UTC (Coordinated Universal Time) and minimum around noon. To extract daily radon patterns, the cluster technique of K-means was applied. Based on this classification, four different case study periods were analyzed in detail, describing two events with high radon levels and two with low radon. Local meteorology, back-trajectories computed with the HYSPLIT (Hybrid Single Particle Lagrangian Integrated Trajectory) model and meteorological fields from the WRF (Weather Research and Forecasting) model, were used to analyze the four case study periods selected. Low radon periods are characterized by the occurrence of non-pure breezes and maritime air masses from the Atlantic Ocean, whereas high radon periods occur under pure sea-land breezes affected by Mediterranean air masses. Factors such as meteorology or local emission sources alone may not be enough to explain the high radon events in the area. Other factors could be playing a major role in the radon levels. The obtained results indicate the contribution of radon transported from medium-long range, suggesting that, under specific weather conditions, the Gulf of Cadiz could act as a radon trap and the continental areas around the Western Mediterranean Basin could act as a radon source.

- Gutiérrez-Álvarez, J.L. Guerrero, J.E. Martín, J.A. Adame, J.P. Bolívar, 2020. Application of hierarchical clustering and FLEXPART-WRF to detect the influence of a NORM repository on the radon concentration in its nearby área. Submission in process.

RESUMEN:
Two radon measurements stations located in two university campus, El Carmen and La Rabida, were used to monitorize radon behavior during the year 2018. The stations were located in the vicinity of Huelva city, in the southwest of Spain, to the north and south of a NORM repository, aiming to detect their influence on the atmospheric radon concentrations of the area through the study of local radon transport events. Hierarchical clustering was employed to identify radon daily patterns. The clustering classification was employed to find four events with interesting features. Atmospheric modelling tools such as WRF and FLEXPART were also used, simulating radon transport in the area on an hourly basis. This approach was able to explain differences in the radon evolution of the stations consistently, pointing out to distinct transport mechanisms that affected each location. The station closer to the NORM repository, El Carmen, was found to be influenced by direct radon diffusion from the repository. The second and further station, La Rabida, was mainly affected by direct radon transport from the NORM repository. These measurements were compared to those of two other coastal stations, finding an average increase of 3.3 Bq m-3 in Huelva, with significant seasonal variations.

7. Conclusions and future lines of research

Radon exhalation and the accumulation chamber method

Two reference exhalation boxes (RB) with a known exhalation rate were made with phosphogypsum from the nearby repository to allow experimenting with the accumulation chamber technique in controlled conditions. These RB were very useful to test accumulation chambers of different sizes connected to different measurement devices. The combination of four measurement devices, 9 accumulation chambers and two fits for the radon growth curve were tested on both reference exhalation boxes:

- All accumulation chambers with some insertion depth provided accurate measurements in the best-case scenario, i.e. using the exponential fit with all available points. The experiments showed that reducing the time available for the radon growth could severely impact the performance of the exponential fit, which required at least 2 to 3 hours to accurately measure the reference exhalation rate.
- The linear fit performance was not adequate in all operational chambers, providing severe underestimations in some cases, even for the shortest accumulation periods. Although this was expected, as the applicability of the linear approximation is only valid when the effective decay constant is low enough, it was proven that linear fit applicability cannot be assumed beforehand, as it is sometimes in the literature, and should be tested and verified for each case.
- A linear relationship between the ratio of perimeter to volume and the effective decay constant suggested that radon transport through the material, under the borders of the accumulators, could have a significant impact on the leaks of the measurement system.
- To study lateral transport, six cylindrical chambers were designed to have the same exhalation surface and accumulation volume but different insertion depths in the PG. The cylindrical chambers proved that lateral radon transport have a deep impact on the effective decay constant of the measurement system. The deeper the insertion length, the smaller the effective decay constant, showing a linear relationship between the logarithm of the effective decay constant and the insertion depth. This could be used to apply the linear approximation for longer accumulation periods, increasing the repeatability and accuracy of the linear fit and reducing the measuring period required.
- This effect was tested and verified on field measurements comparing accumulators with different insertion depths, where an insertion depth of 6 cm was found appropriate in order to provide reliable measurements on the PG repository. Field measurement confirmed that lateral diffusion plays a crucial role in the accumulation chamber method, forcing the practitioner to insert the accumulator into the soil. However, the actual insertion depth would probably depend on the characteristics of the soil, such as porosity, radon diffusion, etc., which will require more experimentation for each material tested.

Atmospheric radon in the city of Huelva

In order to study atmospheric radon behavior in the city of Huelva, several years of radon measurements on the stations of El Carmen and La Rabida were used. General statistics on the daily and monthly variations were carried out, allowing to find high radon periods and relevant atmospheric conditions. Clustering techniques and atmospheric models were employed to study radon daily behavior and its transport, including long-range and local transport.

A first clustering classification with El Carmen station measurements from March 2015 to March 2016 was performed:

- Ambient radon in Huelva shows a seasonal behavior, reaching higher values on autumn than on the rest of the seasons. However, minimal values were similar across the seasons. In all seasons the maximum values registered were 1.5 to 3 times higher than the 95th percentiles of each season, pointing to the appearance of high-radon events with less than 5 % occurrence.
- Higher radon clusters showed a peak centered around dawn, with a first group presenting a narrow high peak followed by a decrease in the morning, and a second group with lesser peak but no effective radon decrease in the afternoon. This last cluster was associated with wind speeds under 2 $m\,s^{-1}$ and lower PBL in the afternoon, which limited the radon purge capacity of the atmosphere.
- The most populated clusters showed flat and low radon concentrations throughout the whole day, forced by higher wind speed during the nighttime that prevented radon increases.
- Four different case studied periods were chosen using this classification, focusing on two high radon events and two low radon events. As expected, local meteorology observations and wind fields simulated by the WRF model confirmed that periods of atmospheric stability help radon to accumulate in the lower layers on the atmosphere.
- HYSPLIT back-trajectories pointed out a possible transport from the Mediterranean Sea, as air masses during high radon periods could be traced to that area. This transport could have two pathways: an indirect transport from the Gulf of Cadiz, entering to the Guadalquivir valley during the day and coming back from NE during the night thanks the breeze pattern, and a direct transport from the Mediterranean Sea across the SE of the Iberian Peninsula, entering first to the low-medium region of the Guadalquivir Valley and reaching the city of Huelva afterwards from NE. Low radon events would be associated with air masses originated in the Atlantic Ocean, having limited or no influence from the Mediterranean Sea.

The second period of study included measurements taken on both FRyMA stations, El Carmen and La Rabida, during 2018. The location of stations with respect to the PG repository, El Carmen to the north and La Rabida to the south, allowed to study local radon transport in detail:

- The general seasonal trends described for El Carmen in 2016 were also observed in the two stations for 2018. Data from the REA network, managed by CSN, were used to compare El Carmen and La Rabida with two coastal stations, Motril and Tarifa, finding significant radon behavior differences between them. On average, Huelva stations have 3 Bq m^{-3} more radon than its other coastal counterparts.
- Clustering analysis showed similar results than those observed in 2016. High radon clusters showed the same two variations: higher radon peak with an effective purging in the afternoon and lesser radon peak with limited purge capacity in the afternoon. The most populated cluster in both stations consisted of almost flat radon activity concentration during the day.
- Although similar, there were differences between stations. El Carmen station showed more days belonging to the first archetype of high radon cluster (higher radon peak, effective afternoon dilution) while La Rabida presented more days related to the latter (lesser radon peak, limited afternoon dilution). There were significantly less days were La Rabida presented days with higher radon cluster assignation than El Carmen. This suggested the influence of a local source in the area, as long-range transport would have affected both stations in the same way.
- Four events were chosen, according to the differences between the stations, and FLEXPART-WRF was used to simulate radon transport with the PG repository acting as a local source. The events showed that radon requires direct transport to reach La Rabida station while El Carmen only required atmospheric stagnant conditions. Thus, local transport appears as the main source

of radon in the area, limiting the possible influence of the long-range transport from the Mediterranean Sea previously studied.

Future lines of research

The research carried out during this thesis points out to future lines of research, such as:

- Design of a radon exhalation calibration system using the reference exhalation boxes. This system could be improved and employed to calibrate measurement system for radon exhalation devices in the future.
- Development of the reference exhalation system to simulate changes in the environmental conditions during exhalation measurements, such as temperature, pressure or humidity. This could help to improve the knowledge about the exhalation behavior during different conditions.
- Measurement of the influence of the insertion depth of the accumulation chamber technique in different types of soils.
- Study of the exhalation variability in the PG stacks, or other soils, using the improved accumulation chambers.
- Once the daily or seasonal variability of the exhalation rate of the PG repository is known, it could be used in transport models such as WRF-CHEM or FLEXPART to simulate the radon transport in the area.
- Use of the clustering technique to study other atmospheric gases such as NO, NO_2 or CO, among others.

References

Abo-Elmagd, M. (2014) 'Radon exhalation rates corrected for leakage and back diffusion – Evaluation of radon chambers and radon sources with application to ceramic tile', *Journal of Radiation Research and Applied Sciences*. Elsevier Ltd, 7(4), pp. 390–398. doi: 10.1016/j.jrras.2014.07.001.

Abril, J. M., García-Tenorio, R. and Manjón, G. (2009) 'Extensive radioactive characterization of a phosphogypsum stack in SW Spain: 226Ra, 238U, 210Po concentrations and 222Rn exhalation rate', *Journal of Hazardous Materials*. Elsevier, 164(2–3), pp. 790–797. doi: 10.1016/J.JHAZMAT.2008.08.078.

Adame, J. A., Serrano, E., *et al.* (2010) 'On the Tropospheric Ozone Variations in a Coastal Area of Southwestern Europe under a Mesoscale Circulation', *Journal of Applied Meteorology and Climatology*, 49(4), pp. 748–759. doi: 10.1175/2009JAMC2097.1.

Adame, J. A., Bolívar, J. P., *et al.* (2010) 'Surface ozone measurements in the southwest of the Iberian Peninsula (Huelva, Spain)', *Environ Sci Pollut Res*, 17, pp. 355–368. doi: 10.1007/s11356-008-0098-9.

Adame, J. A. *et al.* (2012) 'Application of cluster analysis to surface ozone, NO 2 and SO 2 daily patterns in an industrial area in Central-Southern Spain measured with a DOAS system', *Science of the Total Environment*, 429, pp. 281–291. doi: 10.1016/j.scitotenv.2012.04.032.

Al-Zoughool, M. and Krewski, D. (2009) 'Health effects of radon: A review of the literature', *International Journal of Radiation Biology*. Taylor & Francis, pp. 57–69. doi: 10.1080/09553000802635054.

Aldenkamp, F. J. (Kernfysisch V. I. *et al.* (1992) 'An assesment of in situ radon exhalation measurements and the relation between free and bound exhalation rates', *Radiation Protection Dosimetry1*, 45(Nuclear Technology Publishing), pp. 449–453.

Alharbi, S. H. and Akber, R. A. (2014) 'Radon-222 activity flux measurement using activated charcoal canisters: Revisiting the methodology', *Journal of Environmental Radioactivity*. Elsevier Ltd, 129, pp. 94–99. doi: 10.1016/j.jenvrad.2013.12.021.

Amgarou, K. (2003) *Long-term measurements of indoor Radon and its progeny in the presence of Thoron using nuclear track detectors a novel approach*, *TDX (Tesis Doctorals en Xarxa)*. Universitat Autònoma de Barcelona. Available at: https://ddd.uab.cat/record/37276 (Accessed: 5 March 2020).

Arasa, R. *et al.* (2016) 'Defining a Standard Methodology to Obtain Optimum WRF Configuration for Operational Forecast: Application over the Port of Huelva (Southern Spain)', *Atmospheric and Climate Sciences*, 06(02), pp. 329–350. doi: 10.4236/acs.2016.62028.

Arnold, D. *et al.* (2010) 'Analysis of radon origin by backward atmospheric transport modelling', *Atmospheric Environment*, 44(4), pp. 494–502. doi: 10.1016/j.atmosenv.2009.11.003.

Beaver, S. and Palazoğlu, A. (2006) 'A cluster aggregation scheme for ozone episode selection in the San Francisco, CA Bay Area', *Atmospheric Environment*. Pergamon, 40(4), pp. 713–725. doi: 10.1016/J.ATMOSENV.2005.10.003.

Bertin Technologies (2019) 'AlphaGUARD User Manual', p. 113.

Birchall, A. and James, A. C. (1994) 'Uncertainty Analysis of the Effective Dose per Unit Exposure from Radon Progeny and Implications for ICRP Risk-Weighting Factors', *Radiation Protection Dosimetry*. Oxford Academic, 53(1–4), pp. 133–140. doi: 10.1093/RPD/53.1-4.133.

Bolívar, J. P. *et al.* (2009) 'Behaviour and fluxes of natural radionuclides in the production process of a phosphoric acid plant', *Applied Radiation and Isotopes*. Pergamon, 67(2), pp. 345–356. doi: 10.1016/J.APRADISO.2008.10.012.

Bolívar, J. P., García-Tenorio, R. and García-León, M. (1995) 'Enhancement of natural radioactivity in soils and salt-marshes surrounding a non-nuclear industrial complex', *Science of The Total Environment*. Elsevier, 173–174, pp. 125–136. doi: 10.1016/0048-9697(95)04735-2.

Bolívar, J. P., García-Tenorio, R. and García-León, M. (1996a) 'On the fractionation of natural radioactivity in the production of phosphoric acid by the wet acid method', *Journal of Radioanalytical and Nuclear Chemistry Letters*, 214(2), pp. 77–88. doi: 10.1007/BF02164808.

Bolívar, J. P., García-Tenorio, R. and García-León, M. (1996b) 'Radioactive impact of some phosphogypsum piles in soils and salt marshes evaluated by γ-ray spectrometry', *Applied Radiation and Isotopes*. Pergamon, 47(9–10), pp. 1069–1075. doi: 10.1016/S0969-8043(96)00108-X.

Bollhöfer, A. and Doering, C. (2016) 'Long-term temporal variability of the radon-222 exhalation flux from a landform covered by low uranium grade waste rock', *Journal of Environmental Radioactivity*, 151, pp. 593–600. doi: 10.1016/j.jenvrad.2015.06.005.

Borge, R. *et al.* (2008) 'A comprehensive sensitivity analysis of the WRF model for air quality applications over the Iberian Peninsula', *Atmospheric Environment*, 42(37), pp. 8560–8574. doi: 10.1016/j.atmosenv.2008.08.032.

Botha, R. *et al.* (2018) 'Characterising fifteen years of continuous atmospheric radon activity observations at Cape Point (South Africa)', *Atmospheric Environment*. Pergamon, 176, pp. 30–39. doi: 10.1016/J.ATMOSENV.2017.12.010.

Brioude, J. *et al.* (2013) 'The Lagrangian particle dispersion model FLEXPART-WRF version 3.1', *Geoscientific Model Development*, 6(6), pp. 1889–1904. doi: 10.5194/gmd-6-1889-2013.

Burton, W. M. and Stewart, N. G. (1960) 'Use of Long-Lived Natural Radioactivity as an Atmospheric Tracer', *Nature*. Nature Publishing Group, 186(4725), pp. 584–589. doi: 10.1038/186584a0.

Butterweck-Dempewolf, G. and Schuler, C. (1996) 'An extended radon chamber model', *Environmental International*, 22(Knutson 1988), pp. 891–898.

Chambers, S. D. *et al.* (2011) 'Separating remote fetch and local mixing influences on vertical radon measurements in the lower atmosphere', *Tellus B: Chemical and Physical Meteorology*. Blackwell Publishing Ltd, 63(5), pp. 843–859. doi: 10.1111/j.1600-0889.2011.00565.x.

Chambers, S. D. *et al.* (2015) 'Quantifying the influences of atmospheric stability on air pollution in Lanzhou, China, using a radon-based stability monitor', *Atmospheric Environment*. Pergamon, 107, pp. 233–243. doi: 10.1016/J.ATMOSENV.2015.02.016.

Chambers, S. D. *et al.* (2016) 'Towards a Universal Baseline Characterisation of Air Masses for High-and Low-Altitude Observing Stations Using Radon-222', *Aerosol and Air Quality Research*, 16, pp. 885–899. doi: 10.4209/aaqr.2015.06.0391.

Chao, C. Y. H. and Tung, T. C. W. (1999) 'Radon Emanation of Building Material—Impace of Back Diffusion and Difference Between One-Dimensional and Three-Dimensional Tests', *Health Physics*, 76(6), pp. 675–681. doi: 10.1097/00004032-199906000-00011.

Chen, Z. *et al.* (2018) 'Radon emission from soil gases in the active fault zones in the Capital of China and its environmental effects', *Scientific Reports*, 8(1), pp. 1–12. doi: 10.1038/s41598-018-35262-1.

Consejo de Seguridad Nuclear (2009) *Red de estaciones automáticas de vigilancia radiológica ambiental (REA) del CSN Colección Informes Técnicos*. Available at: https://www.csn.es/documents/10182/27786/INT-04-18+Red+de+estaciones+automáticas+de+vigilancia+radiológica+ambiental+%28REA%29+del+CSN.+Operación+y+resultados.+Años+2006+y+2007 (Accessed: 16 March 2018).

Crawford, J. *et al.* (2013) 'Estimating the near-surface daily fine aerosol load using hourly Radon-222 observations', *Atmospheric Pollution Research*. Elsevier, 4(1), pp. 1–13. doi: 10.5094/APR.2013.001.

Crawford, J. *et al.* (2015) 'Using Radon-222 as an Indicator of Atmospheric Mixing Depth in ME-2 for PM 2.5 Source Apportionment', *Aerosol and Air Quality Research*, 15, pp. 611–624. doi: 10.4209/aaqr.2014.11.0303.

Cristofanelli, P. *et al.* (2015) 'Long-term surface ozone variability at Mt. Cimone WMO/GAW global station (2165 m a.s.l., Italy)', *Atmospheric Environment*. Pergamon, 101, pp. 23–33. doi: 10.1016/J.ATMOSENV.2014.11.012.

Darby, S. *et al.* (2005) 'Radon in homes and risk of lung cancer: Collaborative analysis of individual data from 13 European case-control studies', *British Medical Journal*. BMJ Publishing Group, 330(7485), pp. 223–226. doi: 10.1136/bmj.38308.477650.63.

Dee, D. P. *et al.* (2011) 'The ERA-Interim reanalysis: configuration and performance of the data assimilation system', *Quarterly Journal of the Royal Meteorological Society*. John Wiley & Sons, Ltd., 137(656), pp. 553–597. doi: 10.1002/qj.828.

Domínguez-López, D. *et al.* (2014) 'Spatial and temporal variation of surface ozone, NO and NO2 at urban, suburban, rural and industrial sites in the southwest of the Iberian Peninsula', *Environmental Monitoring and Assessment*. Kluwer Academic Publishers, 186(9), pp. 5337–5351. doi: 10.1007/s10661-014-3783-9.

Draxler, R. *et al.* (2018) *HYSPLIT4 User's Guide*. Available at: https://www.arl.noaa.gov/documents/reports/hysplit_user_guide.pdf (Accessed: 3 July 2018).

Dudhia, J. and Wang, W. (2014) 'WRF Advanced Usage and Best practices', p. 35.

Dueñas, C. *et al.* (1997) 'Release of 222Rn from some soils', *Annales Geophysicae*. Springer-Verlag, 15(1), pp. 124–133. doi: 10.1007/s00585-997-0124-0.

Dueñas, C. *et al.* (2007) 'Rn from phosphogypsum piles located at the Southwest of Spain', *Journal of Environmental Radioactivity*, 95, pp. 63–74. doi: 10.1016/j.jenvrad.2007.01.012.

European Environment Agency (2011) *The application of models under the European Union's Air Quality Directive: A technical reference guide*. Available at: https://www.eionet.europa.eu/events/EIONET/Technical report_3 (Accessed: 23 March 2018).

Everitt, B. S. *et al.* (2011) *Cluster Analysis*, *Quality and Quantity*. doi: 10.1007/BF00154794.

Faheem, M. and Matiullah (2008) 'Radon exhalation and its dependence on moisture content from samples of soil and building materials', *Radiation Measurements*, 43(8), pp. 1458–1462. doi: 10.1016/j.radmeas.2008.02.023.

Gómez, J. *et al.* (1991) 'Medida de niveles de radon con carbono activo'.

Grossi, C. *et al.* (2012) 'Atmospheric 222Rn concentration and source term at El Arenosillo 100 m meteorological tower in southwest Spain', *Radiation Measurements*. Elsevier Ltd, 47(2), pp. 149–162. doi: 10.1016/j.radmeas.2011.11.006.

Grossi, C. *et al.* (2016) 'Analysis of ground-based 222 Rn measurements over Spain: Filling the gap in southwestern Europe', *Journal of Geophysical Research: Atmospheres*, 121, pp. 11021–11037. doi: 10.1002/2016JD025196.

Grossi, C. *et al.* (2018) 'Study of the daily and seasonal atmospheric CH4 mixing ratio variability in a rural Spanish region using 222Rn tracer', *Atmospheric Chemistry and Physics*, 18(8), pp. 5847–5860. doi: 10.5194/acp-18-5847-2018.

Grossi, C., Vargas, A. and Arnold, D. (2008) 'C. Grossi et al. Quality study of electret radon flux monitors by an in situ intercomparison campaign in spain', in *Sources and Measurements of Radon and Radon Progeny Applied to Climate and Air Quality Studies*. Vienna: International Atomic Energy Agency, pp. 39–48.

Gutiérrez-Álvarez, I. *et al.* (2020) 'Applicability of the closed-circuit accumulation chamber technique to measure radon surface exhalation rate under laboratory conditions', *Radiation Measurements*. Elsevier Ltd, 133, p. 106284. doi: 10.1016/j.radmeas.2020.106284.

Hernández-Ceballos, M. A. (2012) *Caracterización meteorológica y modelización de Andalucía occidental*. University of Huelva.

Hernández-Ceballos, M. A. *et al.* (2015) 'The role of mesoscale meteorology in modulating the ^{222}Rn concentrations in Huelva (Spain) - impact of phosphogypsum piles', *Journal of Environmental Radioactivity*, 145, pp. 1–9. doi: 10.1016/j.jenvrad.2015.03.023.

Hersbach, H. *et al.* (2020) 'The ERA5 global reanalysis', *Quarterly Journal of the Royal Meteorological Society*. John Wiley and Sons Ltd, 146(730), pp. 1999–2049. doi: 10.1002/qj.3803.

Hirao, S. *et al.* (2008) 'Development and Verification of Long-Range Atmospheric Radon-222 Transport Model', *Journal of Nuclear Science and Technology*, 45(sup6), pp. 166–172. doi: 10.1080/00223131.2008.10876001.

Hong, S.-Y. *et al.* (2006) 'A New Vertical Diffusion Package with an Explicit Treatment of Entrainment Processes', *Monthly Weather Review*, 134(9), pp. 2318–2341. doi: 10.1175/MWR3199.1.

Hosoda, M. *et al.* (2007) 'Effect of Soil Moisture Content on Radon and Thoron Exhalation', *Journal of Nuclear Science and Technology*, 44(4), pp. 664–672. doi: 10.1080/18811248.2007.9711855.

Hosoda, M. *et al.* (2011) 'Development and application of a continuous measurement system for radon exhalation rate', *Review of Scientific Instruments*, 82(1), pp. 1–4. doi: 10.1063/1.3527065.

IAEA (2013) *Technical Report Series No. 474. Measurement and Calculation of Radon Releases from NORM Residues*. Available at: http://www-pub.iaea.org/MTCD/Publications/PDF/trs474_webfile.pdf.

ICRP (1993) 'Protection against radon-222 at home and at work. ICRP Publication 65.', *Ann. ICRP 23(2)*.

ICRP (1994a) 'Dose coefficients for intakes of radionuclides by workers: Coefficients for radionuclides not listed in ICRP Publication 68', *Ann. ICRP 24(4)*. Available at: http://inis.iaea.org/Search/search.aspx?orig_q=RN:31026890 (Accessed: 18 September 2020).

ICRP (1994b) 'Human respiratory tract model for radiological protection. ICRP Publication 66.', *Ann. ICRP 24 (1-3)*.

ICRP (1994c) 'Protection Against Radon-222 at Home and at Work: ICRP Publication 65.', *Ann. ICRP 23(2)*. Oxford.

ICRP (2010) 'Lung Cancer Risk from Radon and Progeny, Part 1. ICRP Publication 115', *Annals of the ICRP 40(1)*.

ICRP (2015) 'Occupational Intakes of Radionuclides: Part 1. ICRP Publication 130', *Ann. ICRP 44(2)*.

ICRP (2017) 'Occupational Intakes of Radionuclides, Part 3. Publication 137', *Ann. ICRP 46(3/4)*.

Ielsch, G. *et al.* (2001) 'Radon (222Rn) level variations on a regional scale: Influence of the basement trace element (U, Th) geochemistry on radon exhalation rates', *Journal of Environmental Radioactivity*, 53(1), pp. 75–90. doi: 10.1016/S0265-931X(00)00106-5.

Iimoto, T. *et al.* (2008) 'Development of a technique for the measurement of the radon exhalation rate using an activated charcoal collector', *Journal of Environmental Radioactivity*, 99(4), pp. 587–595. doi: 10.1016/j.jenvrad.2007.08.024.

ISO (2012) *11665-7:2012 - Measurement of radioactivity in the environment - Air: radon-222 - Part 7: Accumulation method for estimating surface exhalation rate*. Available at: https://www.iso.org/standard/52193.html (Accessed: 27 February 2019).

Jacob, D. J. *et al.* (1997) 'Evaluation and intercomparison of global atmospheric transport models using ^{222} Rn and other short-lived tracers', *Journal of Geophysical Research: Atmospheres*. Wiley-Blackwell, 102(D5), pp. 5953–5970. doi: 10.1029/96JD02955.

James, A. C. *et al.* (1988) 'The Significance of Equilibrium and Attachment in Radon Daughter Dosimetry', *Radiation Protection Dosimetry*. Oxford Academic, 24(1–4), pp. 451–455. doi: 10.1093/oxfordjournals.rpd.a080322.

Janjić, Z. I. (1994) 'The Step-Mountain Eta Coordinate Model: Further Developments of the Convection, Viscous Sublayer, and Turbulence Closure Schemes', *Monthly Weather Review*, 122(5), pp. 927–945. doi: 10.1175/1520-0493(1994)122<0927:TSMECM>2.0.CO;2.

Jónás, J. *et al.* (2017) 'Study of a remediated coal ash depository from a radiological perspective', *Journal of Environmental Radioactivity*, 173, pp. 75–84. doi: 10.1016/j.jenvrad.2016.11.010.

Jonassen, N. (1983) 'The Determination of Radon Exhalation Rates', *Health Physics*, 45(2), pp. 369–376. doi: 10.1097/00004032-198308000-00009.

Karstens, U. *et al.* (2015) 'A process-based ^{222}radon flux map for Europe and its comparison to long-term observations', *Atmospheric Chemistry and Physics*, 15(22), pp. 12845–12865. doi: 10.5194/acp-15-12845-2015.

Keller, G. and Hoffmann, B. (2000) 'The radon diffusion length as a criterion for the radon tightness', *IRPA-10: 10. international congress of the International Radiation Protection Association; Hiroshima (Japan)*, pp. 1–4. Available at: https://inis.iaea.org/search/search.aspx?orig_q=RN:32031528.

Keller, G., Hoffmann, B. and Feigenspan, T. (2001) 'Radon permeability and radon exhalation of building materials.', *The Science of the total environment*, 272(1–3), pp. 85–9. Available at: http://www.ncbi.nlm.nih.gov/pubmed/11379942 (Accessed: 23 January 2019).

Knoll, G. F. (2010) *Radiation Detection and Measurement*. 4th edn. John Wiley & Sons, Ltd.

Kotrappa, P. *et al.* (1990) 'A practical e-perm™ (Electret passive environmental radon monitor) system for indoor222rn measurement', *Health Physics*. Health Phys, 58(4), pp. 461–467. doi: 10.1097/00004032-199004000-00008.

Kotrappa, P. (2015) 'Electret ion chambers for characterizing indoor, outdoor, geologic and other sourced of radon', in. Nova Sciencie Publishers.

Kreuzer, M. *et al.* (2015) 'Lung cancer risk at low radon exposure rates in German uranium miners', *British Journal of Cancer*. Nature Publishing Group, 113(9), pp. 1367–1369. doi: 10.1038/bjc.2015.324.

Kumar, R., Sengupta, D. and Prasad, R. (2003) 'Natural radioactivity and radon exhalation studies of rock samples from Surda Copper deposits in Singhbhum shear zone', *Radiation Measurements*, 36(1-6 SPEC.), pp. 551–553. doi: 10.1016/S1350-4487(03)00201-4.

Leggett, R. *et al.* (2013) 'A generic biokinetic model for noble gases with application to radon', *Journal of Radiological Protection*. J Radiol Prot, 33(2), pp. 413–432. doi: 10.1088/0952-4746/33/2/413.

Levin, I. *et al.* (2002) 'Observations of atmospheric variability and soil exhalation rate of radon-222 at a Russian forest site: Technical approach and deployment for boundary layer studies', *Tellus, Series B: Chemical and Physical Meteorology*, 54(5), pp. 462–475. doi: 10.1034/j.1600-0889.2002.01346.x.

López-Coto, I. *et al.* (2009) 'A short-time method to measure the radon potential of porous materials', *Applied Radiation and Isotopes*, 67, pp. 133–138.

López-Coto, I. (2011) *Variabilidad espacial y temporal de fuentes y concentraciones de radón en la baja atmósfera*. University of Huelva.

López-Coto, I. *et al.* (2014) 'Studying radon exhalation rates variability from phosphogypsum piles in the SW of Spain', *Journal of Hazardous Materials*. Elsevier B.V., 280, pp. 464–471. doi: 10.1016/j.jhazmat.2014.07.025.

López-Coto, I., Mas, J. L. and Bolívar, J. P. (2013) 'A 40-year retrospective European radon flux inventory including climatological variability', *Atmospheric Environment*. Elsevier Ltd, 73, pp. 22–33. doi: 10.1016/j.atmosenv.2013.02.043.

Mas, J. L. *et al.* (2006) 'An assay on the effect of preliminary restoration tasks applied to a large

TENORM wastes disposal in the south-west of Spain', *Science of The Total Environment*, 364(1–3), pp. 55–66. doi: 10.1016/j.scitotenv.2005.11.006.

Mayya, Y. S. (2004) 'Theory of radon exhalation into accumulators placed at the soil-atmosphere interface', *Radiation Protection Dosimetry*, 111(3), pp. 305–318. doi: 10.1093/rpd/nch346.

Mazur, J. and Kozak, K. (2014) 'Complementary system for long term measurements of radon exhalation rate from soil', *Review of Scientific Instruments*, 85(2), pp. 1–7. doi: 10.1063/1.4865156.

Moore, H. E., Poet, S. E. and Martell, E. A. (1973) '222 Rn, 210 Pb, 210 Bi, and 210 Po profiles and aerosol residence times versus altitude', *Journal of Geophysical Research*, 78(30), pp. 7065–7075. doi: 10.1029/JC078i030p07065.

Müllerová, M. *et al.* (2018) 'Study of radon exhalation from the soil', *Journal of Radioanalytical and Nuclear Chemistry*. Springer Netherlands, 315(2), pp. 237–241. doi: 10.1007/s10967-017-5657-4.

Nazaroff, W. W. (1992) 'Radon transport from soil to air', *Reviews of Geophysics*, 30(2), p. 137. doi: 10.1029/92RG00055.

Noverques, A. *et al.* (2019) 'Experimental radon exhalation measurements: Comparison of different techniques', *Radiation Physics and Chemistry*. Elsevier Ltd, 155, pp. 319–322. doi: 10.1016/j.radphyschem.2018.08.002.

Onishchenko, A., Zhukovsky, M. and Bastrikov, V. (2015) 'Calibration system for measuring the radon flux density', *Radiation Protection Dosimetry*, 164(4), pp. 582–586. doi: 10.1093/rpd/ncv315.

Pérez-López, R. *et al.* (2010) 'Dynamics of contaminants in phosphogypsum of the fertilizer industry of Huelva (SW Spain): From phosphate rock ore to the environment', *Applied Geochemistry*. Pergamon, 25(5), pp. 705–715. doi: 10.1016/j.apgeochem.2010.02.003.

Pielke, R. A. (2002) *Mesoscale Meteorological Modeling*, *Mesoscale Meteorological Modeling*. doi: 10.1016/C2009-0-02981-X.

Pisso, I. *et al.* (2019) 'The Lagrangian particle dispersion model FLEXPART version 10.3', *Geoscientific Model Development Discussions*, (January), pp. 1–67. doi: 10.5194/gmd-2018-333.

Planinić, J. *et al.* (1997) 'Radon equilibrium factor and aerosols', *Nuclear Instruments and Methods in Physics Research, Section A: Accelerators, Spectrometers, Detectors and Associated Equipment*. North-Holland, 396(3), pp. 414–417. doi: 10.1016/S0168-9002(97)00707-9.

Pleim, J. E. (2007) 'A Combined Local and Nonlocal Closure Model for the Atmospheric Boundary Layer. Part I: Model Description and Testing', *Journal of Applied Meteorology and Climatology*, 46(9), pp. 1383–1395. doi: 10.1175/JAM2539.1.

Podstawczyńska, A. (2016) 'Differences of near-ground atmospheric Rn-222 concentration between urban and rural area with reference to microclimate diversity', *Atmospheric Environment*. Pergamon, 126, pp. 225–234. doi: 10.1016/J.ATMOSENV.2015.11.037.

Porstendörfer, J. (1994) 'Properties and behaviour of radon and thoron and their decay products in the air', *Journal of Aerosol Science*, 25(2), pp. 219–263. doi: 10.1016/0021-8502(94)90077-9.

Porstendörfer, J. (2001) 'Physical Parameters and Dose Factors of the Radon and Thoron Decay Products', *Radiation Protection Dosimetry*. Nuclear Technology Publishing, 94(4), pp. 365–373. doi:

10.1093/oxfordjournals.rpd.a006512.

Porstendörfer, J., Butterweck, G. and Reineking, A. (1991) 'Diurnal variation of the concentrations of radon and its short-lived daughters in the atmosphere near the ground', *Atmospheric Environment Part A, General Topics*. doi: 10.1016/0960-1686(91)90069-J.

Quindós, L. S. *et al.* (1994) 'Natural radioactivity in spanish soils', *Health Physics*, 66(2), pp. 194–200. doi: 10.1097/00004032-199402000-00010.

Quindós, L. S. *et al.* (2002) 'Medida de la Exhalación de Radón en el Suelo', *Ciencias Nucleares*, 32.

Redeker, K. R., Baird, A. J. and Teh, Y. A. (2015) 'Quantifying wind and pressure effects on trace gas fluxes across the soil–atmosphere interface', *Biogeosciences*, 12(24), pp. 7423–7434. doi: 10.5194/bg-12-7423-2015.

Rogers, V. C. and Nielson, K. K. (1991) 'Multiphase radon generation and transport in porous materials.', *Health Physics*, 60(6), pp. 807–815.

Ryzhakova, N. K. (2012) 'Parameters of modeling radon transfer through soil and methods of their determination', *Journal of Applied Geophysics*. Elsevier B.V., 80, pp. 151–157. doi: 10.1016/j.jappgeo.2012.01.010.

Sahoo, B. K. *et al.* (2010) 'Radon exhalation studies in an Indian uranium tailings pile', *Radiation Measurements*. Pergamon, 45(2), pp. 237–241. doi: 10.1016/J.RADMEAS.2010.01.008.

Sahoo, B. K. and Mayya, Y. S. (2010) 'Two dimensional diffusion theory of trace gas emission into soil chambers for flux measurements', *Agricultural and Forest Meteorology*, 150(9), pp. 1211–1224. doi: 10.1016/j.agrformet.2010.05.009.

Sakoda, A., Ishimori, Y. and Yamaoka, K. (2011) 'A comprehensive review of radon emanation measurements for mineral, rock, soil, mill tailing and fly ash', *Applied Radiation and Isotopes*. Elsevier, 69(10), pp. 1422–1435. doi: 10.1016/j.apradiso.2011.06.009.

Sasaki, T., Gunji, Y. and Okuda, T. (2004) 'Mathematical Modeling of Radon Emanation', *Journal of Nuclear Science and Technology*, 41(2), pp. 142–151. doi: 10.1080/18811248.2004.9715470.

Schery, S. D. and Huang, S. (2004) 'An estimate of the global distribution of radon emissions from the ocean', *Geophysical Research Letters*. Wiley-Blackwell, 31(19), p. L19104. doi: 10.1029/2004GL021051.

Seaman, N. L. *et al.* (2009) 'Sensitivity of vertical structure in the stable boundary layer to variations of the WRF model's Mellor-Yamada-Janjic turbulence scheme', in *10th WRF Users' Workshop*. Available at: https://pdfs.semanticscholar.org/40fb/278b8f11742b98bd4b3dab2513b50792328a.pdf (Accessed: 8 February 2018).

Seo, J. *et al.* (2018) 'Standard Measurement Procedure for Soil Radon Exhalation Rate and Its Uncertainty', *Journal of Radiation Protection and Research*, 43(1), pp. 29–38. doi: 10.14407/jrpr.2018.43.1.29.

Seo, S. *et al.* (2019) 'Health effects of exposure to radon: implications of the radon bed mattress incident in Korea', *Epidemiology and health*. NLM (Medline), 41, p. e2019004. doi: 10.4178/epih.e2019004.

Skamarock, C. *et al.* (2008) *A Description of the Advanced Research WRF Version 3*. doi: 10.5065/D68S4MVH.

Spehr, W. and Johnston, A. (1983) 'The measurement of radon emanation rates using activated charcoal', *Radiation protection in Australia*, 1(3), pp. 113–116. Available at: https://inis.iaea.org/search/searchsinglerecord.aspx?recordsFor=SingleRecord&RN=15010522.

Suarez Mahou, E. *et al.* (2000) *Proyecto Marna. Mapa de radiación gamma natural*. Madrid, Spain: Consejo de Seguridad Nuclear (CSN).

Sun, K., Guo, Q. and Zhuo, W. (2004) 'Feasibility for Mapping Radon Exhalation Rate from Soil in China', *Journal of Nuclear Science and Technology*, 41(1), pp. 86–90. doi: 10.1080/18811248.2004.9715462.

Surkov, Y. A. and Fedoseyev, G. A. (1977) 'Radioactivity of the Moon, Planets, and Meteorites', in. United States. Available at: https://ntrs.nasa.gov/search.jsp?R=19780004993.

Tchorz-Trzeciakiewicz, D. E. and Kłos, M. (2017) 'Factors affecting atmospheric radon concentration, human health', *Science of the Total Environment*. Elsevier B.V., 584–585, pp. 911–920. doi: 10.1016/j.scitotenv.2017.01.137.

Toledano, C. *et al.* (2009) 'Airmass Classification and Analysis of Aerosol Types at El Arenosillo (Spain)', *Journal of Applied Meteorology and Climatology*, 48(5), pp. 962–981. doi: 10.1175/2008JAMC2006.1.

Tsapalov, A., Kovler, K. and Miklyaev, P. (2016) 'Open charcoal chamber method for mass measurements of radon exhalation rate from soil surface', *Journal of Environmental Radioactivity*. Elsevier Ltd, 160, pp. 28–35. doi: 10.1016/j.jenvrad.2016.04.016.

UNSCEAR (2000) *Sources and Effects of Ionizing Radiation. Volume I*. United Nations Publication. Available at: http://www.unscear.org/docs/publications/2000/UNSCEAR_2000_Report_Vol.I.pdf.

UNSCEAR (2008) *Sources, Effects and Risks of Ionizing Radiation Vol. I*, *Radiation Research*. doi: 10.2307/3577647.

Vargas, A. *et al.* (2015) 'Analysis of the vertical radon structure at the spanish "El arenosillo" tower station', *Journal of Environmental Radioactivity*, 139, pp. 1–17. doi: 10.1016/j.jenvrad.2014.09.018.

Vargas, A. and Ortega, X. (2006) 'Influence of environmental changes on continuous radon monitors. Results of a Spanish intercomparison exercise', *Radiation Protection Dosimetry*, 121(3), pp. 303–309. doi: 10.1093/rpd/ncl036.

Vargas, A., Ortega, X. and Matarranz, J. L. M. (2004) 'Traceability of radon-222 activity concentration in the radon chamber at the technical university of Catalonia (Spain)', *Nuclear Instruments and Methods in Physics Research, Section A: Accelerators, Spectrometers, Detectors and Associated Equipment*, 526(3), pp. 501–509. doi: 10.1016/j.nima.2004.02.022.

Vaupotič, J. and Kobal, I. (2006) 'Effective doses in schools based on nanosize radon progeny aerosols', *Atmospheric Environment*. Pergamon, 40(39), pp. 7494–7507. doi: 10.1016/j.atmosenv.2006.07.006.

Wilkening, M. H. (1952) 'Natural Radioactivity as a Tracer in the Sorting of Aerosols According to Mobility', *Review of Scientific Instruments*. American Institute of Physics, 23(1), pp. 13–16. doi:

10.1063/1.1746056.

Xie, D. *et al.* (2014) 'Radon dispersion modeling and dose assessment for uranium mine ventilation shaft exhausts under neutral atmospheric stability', *Journal of Environmental Radioactivity*. Elsevier Ltd, 129, pp. 57–62. doi: 10.1016/j.jenvrad.2013.12.003.

Yang, J. *et al.* (2019) 'Modeling of radon exhalation from soil influenced by environmental parameters', *Science of the Total Environment*. Elsevier B.V., 656, pp. 1304–1311. doi: 10.1016/j.scitotenv.2018.11.464.

Yarmoshenko, I. *et al.* (2018) 'Method for measuring radon flux density from soil activated by a pressure gradient', *Radiation Measurements*, 119, pp. 150–154. doi: 10.1016/j.radmeas.2018.10.011.

Zhuo, W., Iida, T. and Furukawa, M. (2006) 'Modeling Radon Flux Density from the Earth's Surface', *Journal of Nuclear Science and Technology*, 43(4), pp. 479–482. doi: 10.1080/18811248.2006.9711127.

Python packages list

CARTOPY Met Office UK. (2013) Cartopy: a cartographic python library with matplotlib support. http://scitools.org.uk/cartopy

DASK Rocklin, M. (2015). Dask: Parallel computation with blocked algorithms and task scheduling. In Proceedings of the 14th python in science conference.

F90NML Ward. M. (2019) f90nml. A Python module for Fortran namelist. The Journal of Open Source Software 4(38), 1474, DOI: http://doi.org/10.21105/joss.01474

FOLIUM Filipe, M. J., & others. (2018). python-visualization/folium: v0.6.0. Zenodo. http://doi.org/10.5281/zenodo.1344457

IPYTHON Pérez, F., & Granger, B. E. (2007). IPython: a system for interactive scientific computing. Computing in Science & Engineering, 9(3).

MATPLOTLIB Hunter, J. D. (2007). Matplotlib: A 2D graphics environment. Computing in Science & Engineering, 9(3), 90–95.

NUMPY Oliphant, T. E. (2006). A guide to NumPy (Vol. 1). Trelgol Publishing USA.

PANDAS McKinney, W., & others. (2010). Data structures for statistical computing in python. In Proceedings of the 9th Python in Science Conference (Vol. 445, pp. 51–56).

SCIPY Virtanen P., & others. (2020) SciPy 1.0: Fundamental Algorithms for Scientific Computing in Python**.** *Nature Methods*, 17(3), 261-272.

SEABORN Waskom, M., & others. (2017). mwaskom/seaborn: v0.8.1 (September 2017). Zenodo. https://doi.org/10.5281/zenodo.883859

TKINTER Lundh, F. (1999). An introduction to tkinter. URL: Www. Pythonware. Com/Library/Tkinter/Introduction/Index. Htm.

XARRAY Hoyer, S. & Hamman, J., (2017). xarray: N-D Labeled Arrays and Datasets in Python. Journal of Open Research Software. 5(1), p.10. DOI: http://doi.org/10.5334/jors.148